



New Avenues for Ligand-Mediated processes – Expanding Metal Reactivity by the use of Redox-Active Catechol, o-Aminophenol and o-Phenylenediamine Ligands

Journal:	<i>Chemical Society Reviews</i>
Manuscript ID:	CS-SYN-02-2015-000161.R2
Article Type:	Review Article
Date Submitted by the Author:	24-Jun-2015
Complete List of Authors:	Broere, Daniel; van t Hoff Institute for Molecular Sciences, Supramolecular + Homogeneous Catalysis Group Plessius, Raoul; van t Hoff Institute for Molecular Sciences, Supramolecular + Homogeneous Catalysis Group van der Vlugt, Jarl Ivar; van t Hoff Institute for Molecular Sciences, Supramolecular + Homogeneous Catalysis Group

New Avenues for Ligand-Mediated processes – Expanding Metal Reactivity by the use of Redox- Active Catechol, *o*-Aminophenol and *o*- Phenylenediamine Ligands

Daniël L. J. Broere, Raoul Plessius, Jarl Ivar van der Vlugt*

Abstract

Redox-active ligands have evolved from being considered spectroscopic curiosities – creating ambiguity about formal oxidation states in metal complexes – to versatile and useful tools to expand on the reactivity of (transition) metals or to even go beyond what is generally perceived possible. This review focusses on metal complexes containing either catechol, *o*-aminophenol or *o*-phenylenediamine type ligands. These ligands have opened up a new area of chemistry for metals across the periodic table. The portfolio of ligand-based reactivity invoked by these redox-active entities will be discussed. This ranges from facilitating oxidative additions upon d^0 metals or cross coupling reactions with cobalt(III) without metal oxidation state changes - by functioning as an electron reservoir - to intramolecular ligand-to-substrate single-electron transfer to create a reactive substrate-centered radical in a palladium complex. Although the current state-of-art research primarily consists of stoichiometric and exploratory reactions, several notable reports of catalysis facilitated by the redox-activity of the ligand will also be discussed. In conclusion, redox-active ligands containing catechol, *o*-aminophenol or *o*-phenylenediamine moieties show great potential to be exploited as reversible electron reservoirs, donating or accepting electrons to activate substrates and metal centers and to enable new reactivity with both early and late transition as well as main group metals.

1. Introduction

The ability of a metal to change oxidation states during metal-mediated chemical transformations has resulted in the use of these metals for catalytic processes. For example, the ability of palladium to undergo two-electron changes (Pd^0/Pd^{II} or Pd^{II}/Pd^{IV}) has resulted in the widespread implementation of Pd-catalyzed cross-coupling reactions.¹ On the other hand, the lack of d-electrons, required to facilitate β -H elimination, in Ti^{IV} , Zr^{IV} and Hf^{IV} complexes make these species highly useful as alkene polymerization catalysts.² Generally speaking, catalytic processes can be distinguished in reductive,

oxidative or redox-neutral processes. Many (industrially relevant) reactions, even when formally redox-neutral, involve two-electron redox-steps and are thus linked to e.g. 2nd and 3rd row (noble) transition metals. Base metals generally prefer to undergo one-electron redox-events but controlled ('metal-mediated') odd-electron pathways are still less commonly encountered, although there is a great interest in the use of abundant, cheap and non-toxic materials. Moreover, the development of unprecedented types of reactivity – which could facilitate or significantly shorten the synthesis of highly desired molecules – is also sought after. Redox-active ligands have shown to be able to do both by working in synergy with the metal and thereby expanding upon a metal's "common" reactivity.³

a) Redox-active ligands

With regular spectator or "redox-inactive" ligands the energy required for oxidation or reduction by one electron is much bigger than that needed to change the oxidation state of the metal. As a consequence, the changes in electronic structure occur at the metal and not at the coordinated ligands (Figure 1, top). Redox-active ligands have more energetically accessible levels for reduction or oxidation.⁴ As a result, either solely ligand-centered redox processes can occur, with the metal center remaining in the same oxidation state (Figure 1, bottom) or both the ligand and metal change oxidation state in a synergistic fashion, creating ambiguity about the electronic state of both metal and ligand. Nature employs this feature in various metalloenzymes wherein the active site contains a redox-active ligand that works in synergy with a metal ion.⁵ This way multi-electron reactions are broken down into smaller steps, avoiding overpotentials and making it possible to work near thermodynamic potential.^{3d}

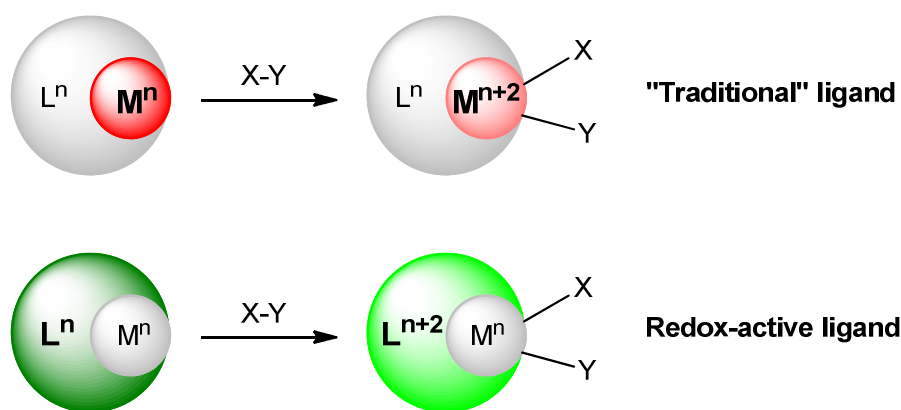


Figure 1 Top: "Traditional" unreactive ligand in an oxidative addition reaction where the metal changes oxidation state. Bottom: Redox-active ligand functioning as an electron reservoir in an oxidative addition reaction thereby keeping the metal in the same oxidation state.

Chemists have identified the principles of redox-active ligands several decades ago but until recently these entities were mainly considered as spectroscopic curiosities. We have decided to refrain from a complete historic perspective including seminal early breakthroughs, but the interested reader is

referred to recent reviews on these aspects.⁶ The true potential of these ligands extends well-beyond the mere identification of non-trivial electronic structure configurations. These ligands can expand metal reactivity in several ways (Figure 2) by A) acting as an electron reservoir, B) modifying the Lewis acidity of the metal, C) generating reactive ligand-centered radicals⁷ that are involved in bond-making and -breaking or D) transferring a single electron to the substrate, which in turn may act as redox-active moiety.

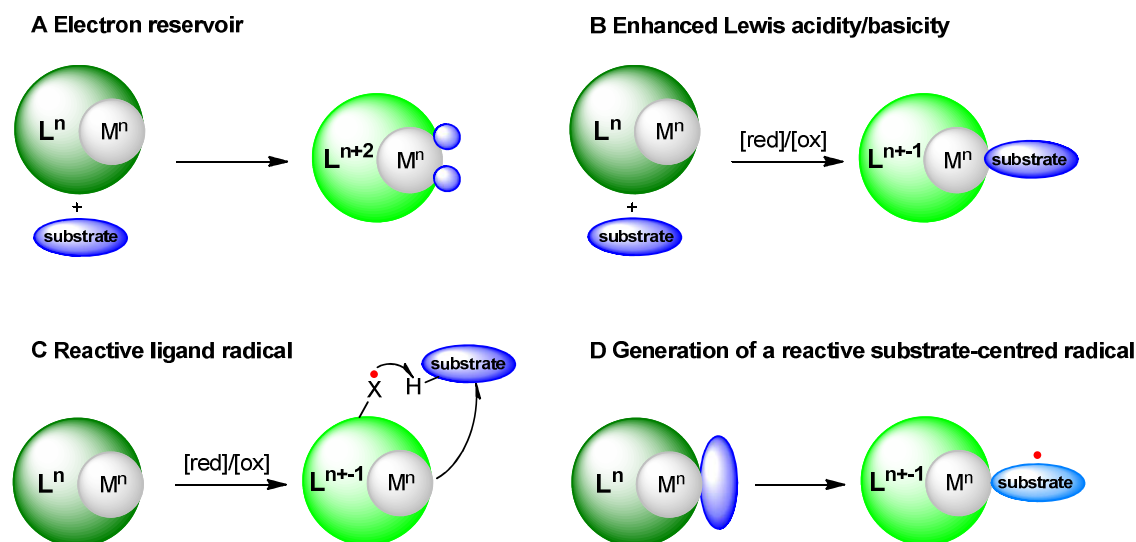


Figure 2 Different ways of how a redox-active ligand can expand the reactivity of a metal center. A) enhancing the Lewis acidity/basicity upon oxidation or reduction; B) functioning as an electron reservoir; C) generation of a reactive ligand radical involved in bond making/breaking reactions; D) generation of a reactive substrate-centered radical.

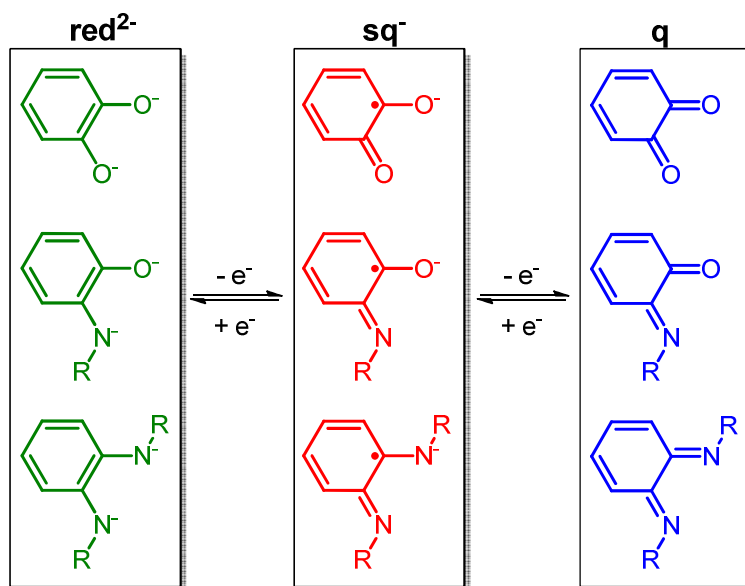
Various classes of redox-active ligands have been developed and (intensely) investigated in the last decades, including applications in catalysis⁸ and material science.⁹ However, the focus in this review is solely on catechol-, *o*-aminophenol- and *o*-phenylenediamine-derived ligands and the processes by which these ligands can adjust, alter or bypass the stoichiometric or catalytic reactivity of a (transition) metal (Scheme 1).



Scheme 1 From left to right: catecholato, *o*-amidophenolato and *o*-phenylenediamido moiety.

These ligands can coordinate to a metal in three different oxidation states for which several different abbreviations can be found throughout the literature. To avoid confusion, in this review we will use the following: **red**²⁻ for the catecholato (cat), amidophenolato (ap) and *o*-phenylenediamido (pda) oxidation state; **sq**⁻ for the semiquinonato (sq), iminosemiquinonato (isq) and *o*-diiminosemiquinonato

(disq)oxidation state; **q** for the quinone (q), iminobenzoquinone (ibq) and *o*-diiminoquinone (diq) oxidation state (scheme 2). The phenyl backbone of these ligands is often substituted to prevent undesired reactivity at the ring in the different oxidation states or to tune the electronic properties. The coordination behavior of these ligands in their different oxidation states has been studied in great detail.^{10,11,12} Very recently, Pinter and de Proft and co-workers reported a DFT study concerning such quinoid related ligand frameworks, which revealed that strengthening of the metal-ligand bonds upon ligand reduction, resulting in stabilized $M-L^{-1/2}$ configurations, strongly contributes to the overall thermodynamically favourable driving force for ligand-centered electron transfer.¹³



Scheme 2 The three possible oxidation states of the catechol-, aminophenol- and *o*-phenylenediamine-derived ligands.

b) Identification of the ligand oxidation state

In most cases, the different oxidation states **red²⁻**, **sq⁻** and **q** can be attained by stepwise chemical or electrochemical one-electron oxidation or reduction. However, it is difficult to predict the resulting oxidation state of a redox-active ligand when combined with a metal because upon coordination, depending on the conditions, all three ligand oxidation states may be accessible. Several analytical techniques are available to determine the oxidation state of both the redox-active ligand and the metal ion. Cyclic voltammetry (Figure 3) provides insight in the potential window for the various metal and ligand-based transitions but is not trivial to determine the locus of the redox-event in this manner.

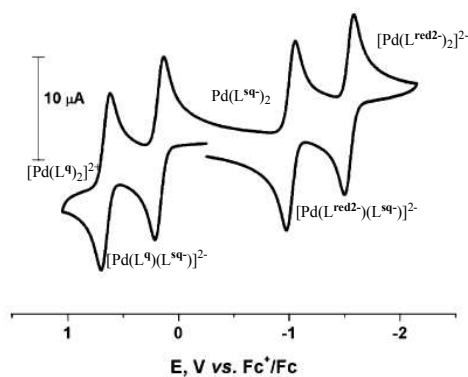
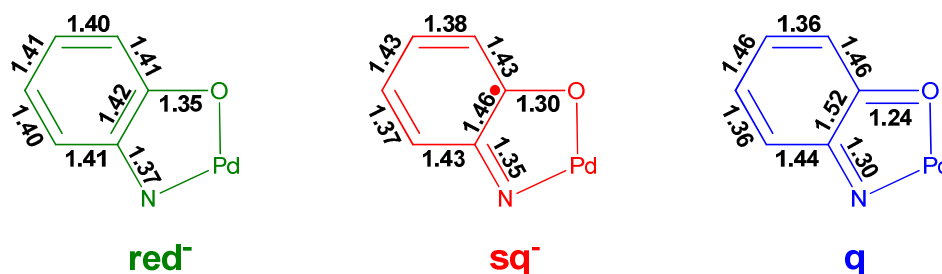


Figure 3 Cyclic voltammogram of a homoleptic Pd(II) complex bearing two redox active amidophenolate ligands in the sq^- oxidation state showing the ease of accessing the different ligand oxidation states. Measured in CH_2Cl_2 solution containing 0.10 M $[\text{N}(\text{n-bu})_4]\text{PF}_6$ as supporting electrolyte with a glassy carbon working electrode at a scan rate of 100 mV s^{-1} with ferrocene as an internal standard. Reprinted with permission granted by the American Chemical Society.¹⁴

Magnetic susceptibility measurements (solid state or in solution) can provide information about the spin-state of the complex and hence the number of unpaired electrons. Single crystal X-ray diffraction of a compound is often informative, as the carbon-carbon bonds of the phenyl ring undergo significant changes upon reduction or oxidation (Scheme 3). However, because these measurements are usually performed at low temperatures only, temperature dependent spin-state changes may be overlooked. Based on a comprehensive analysis of structural data, Brown has developed a method that allows for the quantification of the oxidation state for aminophenolate and catecholate derived ligands.¹⁵ Using this method a “metrical oxidation state” (MOS) can be assigned based on the C-C, C-O and C-N bond bond lengths using a simple Microsoft Excel spreadsheet provided in the supporting information of Browns article. High-valent d^0 complexes can give unexpectedly positive MOS values that are not attributed to electron transfer but to ligand-to-metal π bonding. Variable temperature magnetic susceptibility measurements using a SQUID magnetometer are useful to address this phenomenon. UV-vis spectroscopy may also provide information about the oxidation state of the redox-active ligand, as transitions may be characteristic for and related to specific oxidation states. Spectroelectrochemistry (either UV-vis or IR) in an optically transparent thin-layer electrolysis (OTTLE) cell can provide information about the reversibility of redox events, whether a redox event is metal or ligand centered and about the potential required for bulk electrolysis.¹⁶ EPR spectroscopy in combination with density functional theory (DFT) calculations will provide information about the location of the unpaired electron(s), especially for the sq^- oxidation state. Less often encountered (but still very useful) analysis methods are X-ray absorption spectroscopy, Mössbauer spectroscopy and magnetic circular dichroism (MCD) in combination with time-dependent DFT calculations.¹⁷



Scheme 3 Characteristic metric parameters for three isostructural Pd(II) complexes in the possible ligand oxidation states displaying the dearomatization upon oxidation.¹⁴

c) Outline

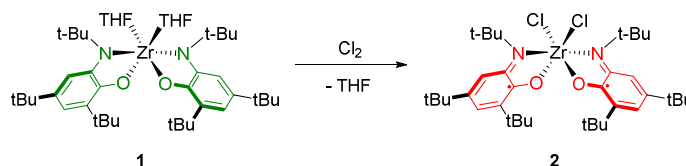
The coordination chemistry and spectroscopy of catechol-, aminophenol- and *o*-phenylenediamine-derived redox-active ligands continues to be extensively explored. This review will focus on complexes with these types of redox-active ligands that are exploited for (catalytic) reactivity studies. A division between the use of redox-active ligands solely as electron reservoirs or as a strategy to alter or expand the reactivity at the metal center or a bound substrate is made. A further subdivision into early transition metals, late transition metals and other metals is presented, showing how redox-active ligands affect the reactivity for each of these metal classes. Throughout the literature the non-equivalent terms “noninnocent”¹⁸ and “redox-active” are used interchangeably. However, in this review the term “redox-active” will be used because in most discussed cases there is no ambiguity regarding the formal oxidation states of the metal or ligands (the term noninnocent was originally coined for such cases).¹⁹

2) Redox-Active Ligands as Electron Reservoir

a) Early Transition metals

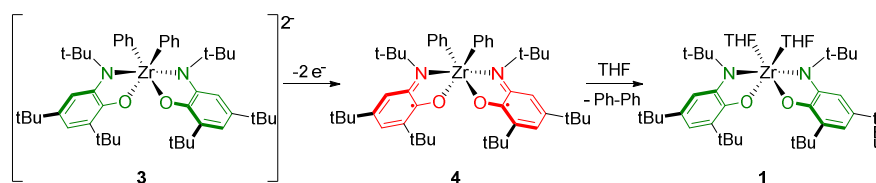
For a metal to be able to undergo β -hydrogen elimination, a vacant site must be accessible and the metal should possess available d-electrons. Early transition metals often occur as completely oxidized (high-valent) metal ions with a d^0 configuration. This explains the abundance of polymerization catalysts based on these high-valent early transition metals, as β -hydrogen elimination is a common termination pathway in polymerization mechanisms. However, the d^0 situation also limits the application of high-valent group 3-5 metals in selective bond functionalization reactions. Oxidative addition is, traditionally, thought to be impossible for d^0 metal ions. Redox-active ligands are powerful tools to confer new reactivity onto early transition metal complexes, provided that the redox-properties can be tuned to accommodate electron transfer to or from the ligand scaffold. For example, for tridentate NNN ligands bearing a redox-active phenylenediamine core and a flanking anilide donor, it was shown that alterations in the backbone substituents allowed for redox potential changes by at least 270 mV.²⁰

An early example of this chemistry was reported by the group of Heyduk, who described a reaction between a (d^0) zirconium(IV) complex (**1**) and molecular chlorine, which resulted in oxidative addition to yield the Zr(IV) dichlorido-derivative (**2**) (Scheme 4).²¹ The presence of two redox-active NO-ligands in the **red**²⁻ amidophenolate oxidation state proves essential for the reactivity of **1**. Upon interaction of the Zr-species with Cl₂, both redox-active ligands are oxidized to the **sq**⁻ oxidation state, thereby donating one electron in order to facilitate homolytic activation of Cl₂. The change in ligand oxidation state was supported by UV-vis and EPR spectroscopy and by comparison of the metric parameters of **1** and **2** obtained from X-ray diffraction. Variable temperature magnetic susceptibility measurements showed that the effective magnetic moment of **2** approaches zero at low temperatures, indicative of a singlet ($S = 0$) diradical ground state, with anti-ferromagnetic coupling between the two ligand radicals. This reaction is an important proof-of-principle that redox-active ligands can act as an electron reservoir to enable reactions that were previously thought to be impossible.



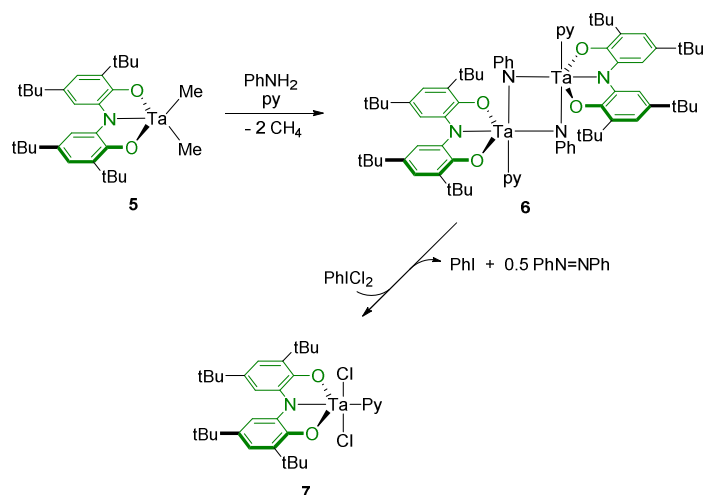
Scheme 4 Ligand-facilitated oxidative addition of molecular chlorine to a zirconium(IV) bis-amidophenolate complex.

The same group also showed that aminophenol-based ligands are also capable of facilitating a formal reductive elimination of a C-C bond on a metal center with a d^0 electron count.²² Upon two-electron oxidation of the initially obtained dianionic Zr-di(phenyl) species **3** – with both NO ligands in the red^{2-} oxidation state – biphenyl is rapidly generated while the resulting metal complex (**1**) still contains two NO ligands in the red^{2-} oxidation state (Scheme 5). This reaction is proposed to proceed via intermediate **4**, as a characteristic band at λ 740 nm, attributed to the isq^- system, was observed at -78 °C by UV-vis spectroscopy, which is the bis(phenyl) analog of complex **2**. Cross-over experiments with the ditolyl analogue of **3** indicated that the reaction occurs at a single Zr(IV) center and does not involve free organic radicals, as the mixed biaryl compound was not detected. This is the first report of a redox-active ligand-assisted C–C reductive elimination. The Heyduk group reported similar reductive elimination reactivity upon oxidation of a titanium complex bearing a redox-active *o*-phenylenediamine NN ligand.²³



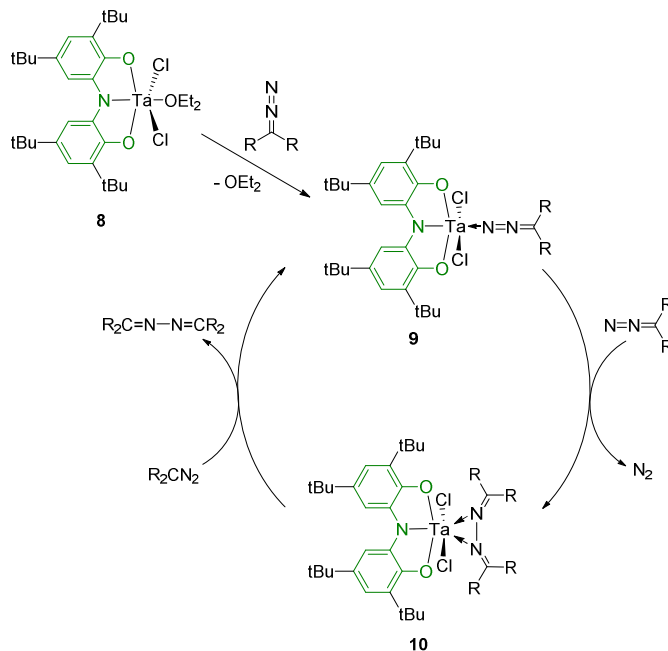
Scheme 5 Ligand-facilitated two electron oxidation followed by reductive elimination of biphenyl on a Zr(IV) complex.

Expanding on this work with early transition metals, tridentate redox-active aminophenol-based ONO ligands bearing an additional donor were found to facilitate unique reactivity.²⁴ Apart from similar oxidative addition reactivity as described for complex **1**, the four-electron oxidative formation of aryl diazenes was achieved (Scheme 6). Reaction of Ta(V) complex **5** with aniline resulted in dinuclear complex **6** with two bridging phenylimido ligands. Oxidation of this species using the two-electron periodinane oxidant dichloriodobenzene led to the formation of diphenyl diazene and Ta(V) complex **7**. The dinuclear Ta_2N_2 core pre-organizes the nitrogen atoms for N=N bond formation, while the redox-active ONO ligands supply the redox-equivalents to facilitate this reaction, being shuttled from red^{2-} to \mathbf{q} before the reductive elimination can occur. Follow-up reactivity of **5** toward arylazides as well as the initial formation of dinuclear complex **6** occurs without involvement of the redox-active ligand.²⁵



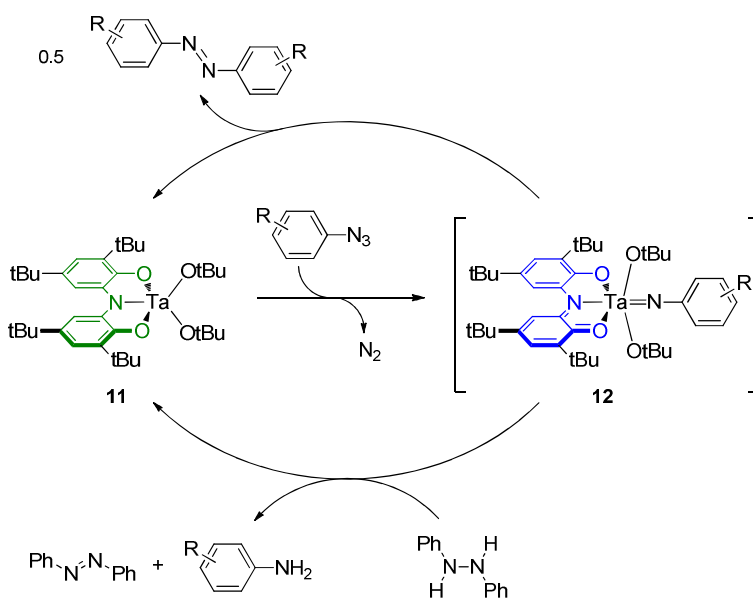
Scheme 6 Four-electron oxidative formation of diazenes facilitated by a Ta(V) complex with a redox-active ONO ligand.

The presence of a potentially redox-active ligand does not automatically imply ligand-based reactivity, as illustrated by the reaction of tantalum(V)dichloro complex **8** with two equivalents of Ph₂CN₂, yielding diphenyl ketazine with the expulsion of dinitrogen (Scheme 7).²⁶ No direct spectroscopic evidence for involvement of the redox-active ligand was found. The proposed catalytic cycle involves coordination of Ph₂CN₂ to form **9**, which after loss of N₂ reacts with another molecule of Ph₂CN₂ to form complex **10**, which could also be isolated. The organic product is released from the metal center upon coordination of exogenous Ph₂CN₂. Moreover, when Ph₂CN₂ was added in neat styrene to complex **8**, the complex was found to catalytically transfer a carbene to styrene.

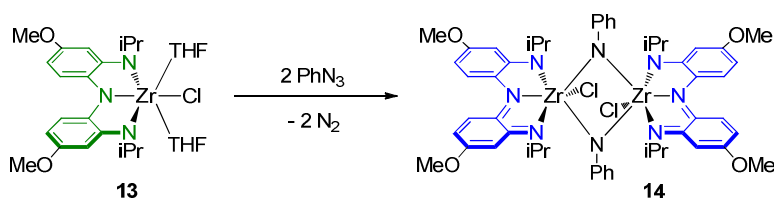


Scheme 7 Catalytic cycle of carbene transfer to form ketazines, using a Ta(V) [ONO] complex. R = Ph.

Dimethyltantalum(V) complex **5** reacts with *t*-butanol to generate dialkyloxyde tantalum(V) complex **11**.²⁷ This species, along with the dichloro analogue,²⁸ is able to react with phenylazide to produce 0.5 equivalents of the corresponding azobenzene in the presence of 1,2-diphenylhydrazine, with intermediacy of tantalum-imido species **12** featuring the ONO ligand in the **q** (iminoquinone) oxidation state (Scheme 8). Unlike the dichloro complex, which decomposes in the presence of excess azide, complex **11** is able to catalytically convert phenylazide to the corresponding azobenzene, albeit with only ten turnovers after seven days at 55 °C. The Zr(NNN) analogue (**13**, Scheme 8), is more easily oxidized (by 200 mV from **red**²⁺ to **sq**⁻ and 300 mV from **sq**⁻ to **q**) and reacts with aryl azides to form imido dimer (**14**). However, unlike with the ONO platform this dimer is indefinitely stable and does not extrude aryldiazene, which is explained by the lower oxidizing ability of the **q** oxidation state (diimine-amide) of the NNN ligand.

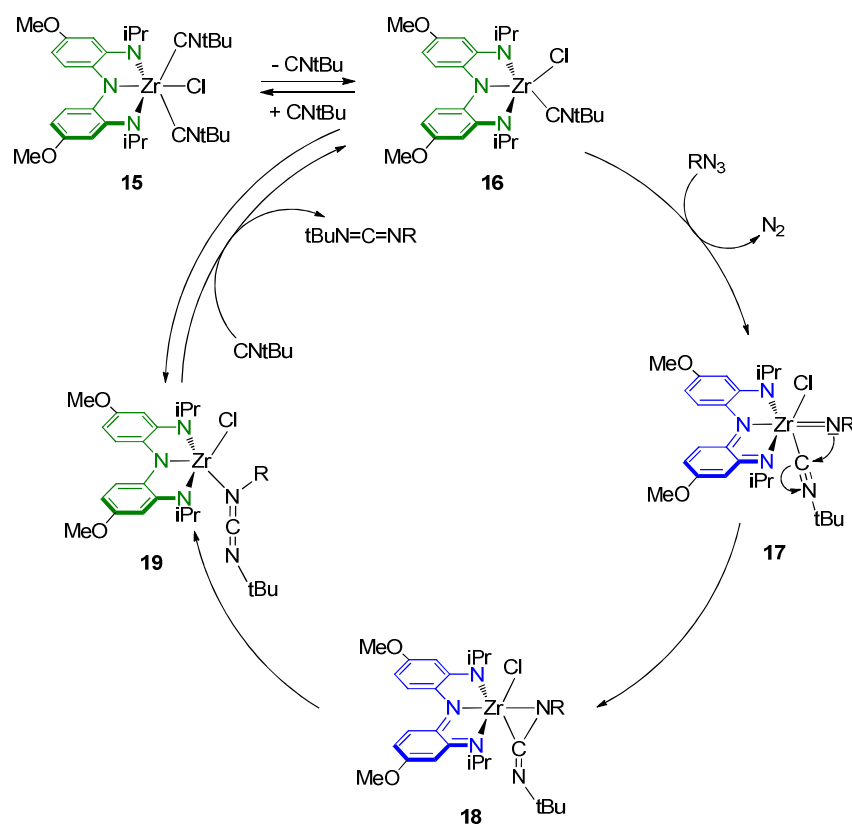


Scheme 8 Nitrene transfer reactions for [(ONO)Ta(Y)₂] complex.



Scheme 9 Reaction of [NNN]ZrCl(THF)₂ with PhN₃ to form an imido dimer.

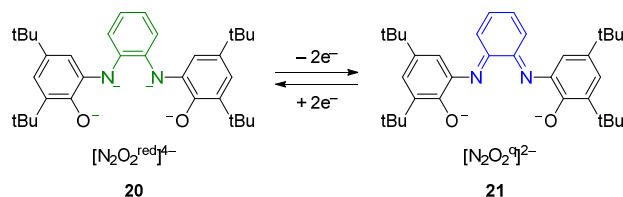
Catalytic nitrene transfer of organoazides to isocyanides to afford carbodiimides was feasible using the related complex **15** (Scheme 9).^{29,30} Complex **15** reacted with one equivalent of the azide 4-*t*BuC₆H₄N₃ (*p*-*tert*-butylphenyl azide) to produce 4-*t*BuC₆H₄N=C=N*t*Bu which expulsion of dinitrogen. Mechanistic investigations led to the proposed mechanism depicted in Scheme 10. Initial dissociation of isonitrile from complex **15** creates five-coordinate species **16**, which reacts with the organoazide to form imido complex **17** with release of N₂. In this step the redox-active NNN ligand is oxidized by two electrons from the **red**²⁻ to the **q** oxidation state. The nitrene group acts as nucleophile upon the electrophilic carbon of the coordinated isocyanide substrate, forming species **18** with a three-membered Zr-C-N metalacycle. Formal reductive elimination of the C=N bond facilitated by two-electron reduction of the NNN ligand to the **red**²⁻ oxidation state produces complex **19**. Reaction with isonitrile releases the carbodiimide product and regenerates complex **16**. With aryl azides, the reaction was halted after two turnovers, but employing alkyl azides such as AdN₃ (Ad = 1-adamantyl) or *t*BuN₃ as substrates provided full conversion after 2 hours at 55 °C with a catalyst loading of 10 mol%.



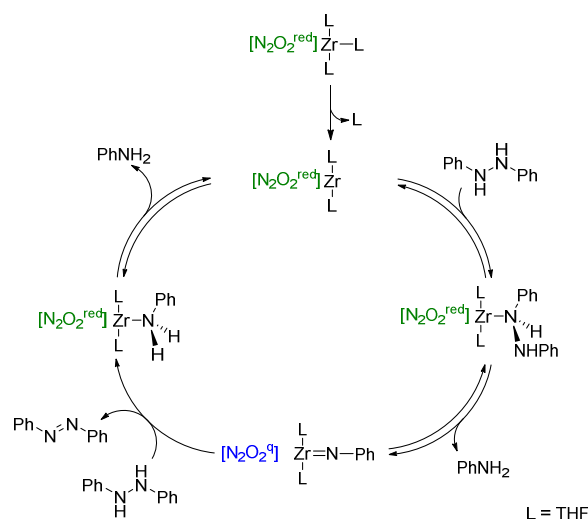
Scheme 10 Catalytic nitrene transfer by [(NNN)ZrCl(CN*t*Bu)₂] complex, yielding carbodiimide 4-*t*BuC₆H₄N=N=*t*Bu.

Recently, a detailed DFT computational study regarding the mechanism of this nitrogen group-transfer reaction was reported by the Baik group.³¹ This study nicely supports the mechanism proposed by Heyduk, as NNN ligand to azido substrate electron transfer was found to be energetically favoured over the classic metal-to-substrate electron transfer pathway. However, the calculated pathway to convert **16** into imido species **17** involves several intermediates. Initial coordination of intact azide is followed by two consecutive, non-concerted ligand-to-substrate single-electron transfer steps. The first ligand-to-substrate electron transfer (concomitant with oxidation of the NNN ligand from the red^{2-} to the sq^- state) generates a one-electron reduced azido fragment that binds side-on via the α - and β nitrogen atoms. N_2 loss is realized only upon oxidation of the ligand from the sq^- to the q state, and **17** is formed. The findings from this computational study are somewhat related to recent findings for ligand-to-substrate single electron transfer with Pd^{II} involving organoazides as substrates, although in that case N_2 loss occurs prior to electron transfer (*vide infra*). Additionally, release of dinitrogen initially generates a stereoisomer of **17** with the nitrene bound *trans* to the isocyanide, which prevents the subsequent intramolecular nucleophilic attack. Hence, the isocyanide needs to dissociate and re-coordinate in a position *cis* to the imido unit for productive nitrogen group-transfer and C-N bond formation to occur. The bonding situation of the Zr-N fragment prior to this step is best described as an imido unit, although the N-transfer is denoted as nitrene group transfer.

Besides bidentate and tridentate ligand scaffolds, aminophenol redox-activity has also been integrated in tetradentate frameworks. The combination of ligand **20** with zirconium(IV) actually led to the first reported case of “two-electron” catalysis with a d^0 metal wherein the redox-active ligand acts as electron reservoir.³² The two oxidation states of the ligand involved in the catalytic cycle are depicted in Scheme 11. As with the Ta(ONO) complex mentioned above, the complex reacted with 1,2-diphenylhydrazine to give one equivalent of azobenzene and two equivalents of aniline instead of a group transfer to the metal. Furthermore, this complex was found to be catalytically competent for this transformation (Scheme 11). The product stoichiometry remains 1:2 even at relatively high substrate-to-catalysts loadings of 100:1 without any side-products being formed. Kinetic experiments showed a first order in both catalyst and 1,2-diphenylhydrazine. Reaction of the starting Zr(**20**) complex with (*p*-tolyl)azide resulted in the formation of a similar dark-green solution as observed under catalytic conditions, which is indicative of the q oxidation state of the ligand.

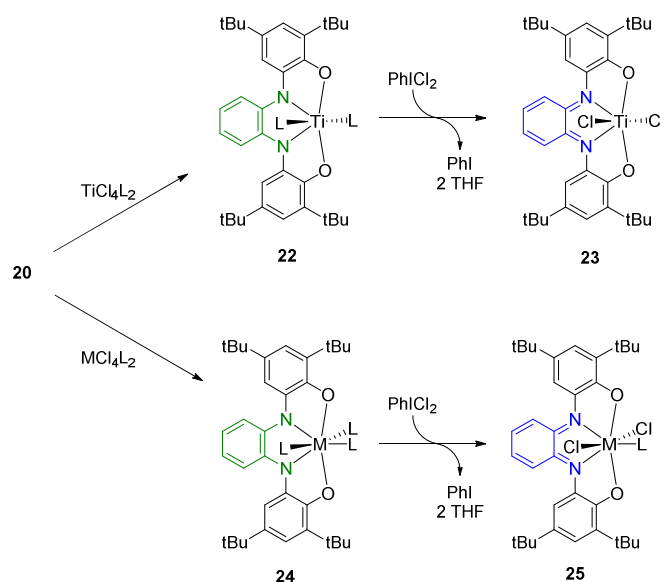


Scheme 11 The two oxidation states of the tetradentate ligand involved in the catalytic group transfer reaction.



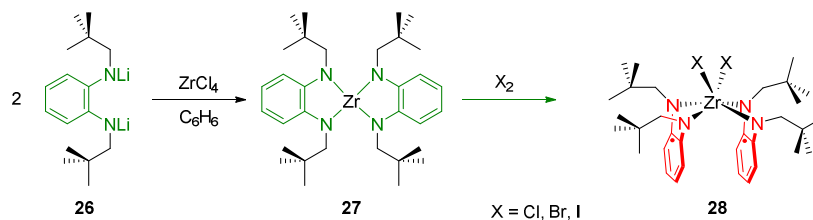
Scheme 12 Catalytic cycle of the $[\text{N}_2\text{O}_2^{\text{red}}]\text{ZrL}_3$ ($\text{L} = \text{THF}$) complex with 1,2-diphenylhydrazine. $[\text{N}_2\text{O}_2^{\text{red}}]$ and $[\text{N}_2\text{O}_2^{\text{ox}}]$ are shown in Scheme 11.

The same tetradentate ligand **20** was later reported to interact with all Group 4 metals in their highest oxidation state, coordinating in a meridional fashion (scheme 13).³³ For zirconium and hafnium (compound **24**), two solvent molecules coordinate axially and a third coordinates in the equatorial plane of the metal, providing overall seven-coordination. For titanium (**22**), only two solvent molecules coordinate, which may be considered to leave a vacant site at the metal center unoccupied that could possibly be exploited for catalytic purposes. In the case of zirconium and hafnium, the equatorial solvent molecule exchanges rapidly with the bulk solvent, also creating possibilities for catalysis. All complexes undergo ‘oxidative addition’ by PhICl_2 to form **23** (Ti) or **25** ($\text{M} = \text{Zr}, \text{Hf}$), facilitated by two-electron oxidation of the redox-active ligand similar to the reactivity depicted in Scheme 4.



Scheme 13 Tetradentate $[N_2O_2]$ coordinated to several different metals (Ti, Zr, Hf) followed by reaction with PhI_2 . L = THF; M = Zr or Hf

Similar redox-active ligand-assisted oxidative addition was found for a tetrahedral zirconium(IV) complex with two phenylenediamide ligands (**27**, Scheme 14).³⁴ Halogens rapidly undergo oxidative addition to generate complex (**28**) featuring two ligand sq^- radicals with the phenyl-backbones of the two ligands adopting a highly unusual π - π stacked conformation. DFT calculations show that the SOMOs of the ligands combine to form a unique bonding HOMO and antibonding LUMO in this conformation. As a result the complex has a closed-shell-singlet ground state ($S = 0$), thus making it susceptible to NMR spectroscopic analysis, which indicated loss of aromaticity. Temperature dependent magnetic susceptibility measurements (using SQUID) showed a thermally accessible triplet state with an estimated singlet-triplet energy gap of 735 cm^{-1} . The combination of these two electrons into a closed-shell electronic structure might be a strategy to favor two-electron reactivity over single-electron reactivity with sq^- platforms.

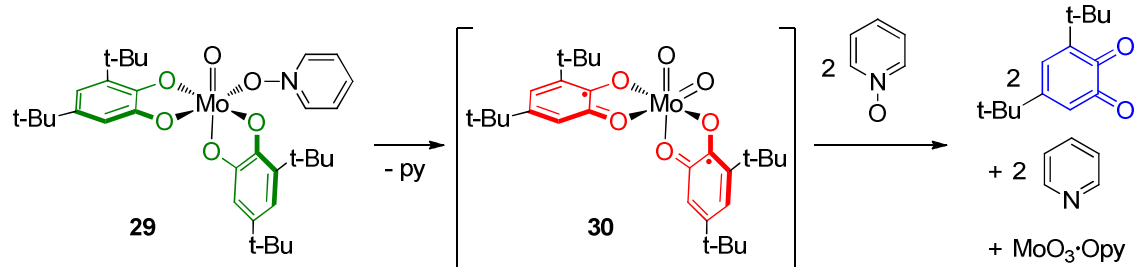


Scheme 14 Synthesis of zirconium(IV) complex **28**, showing unusual π - π stacking. X = Cl, Br or I

More recently, Heyduk *et al.* investigated the effect of the metal atom in a series of three isostructural ONO pincer complexes (V, Nb and Ta).³⁵ The most noteworthy finding is that the DFT calculated ground state of the vanadium complex was best described as an open-shell singlet with one unpaired

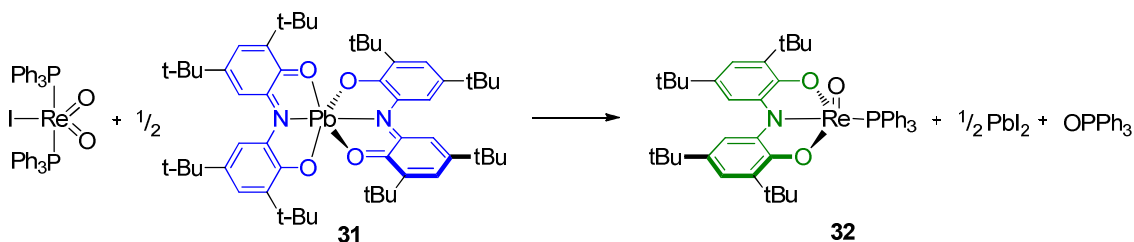
electron on the ligand and one on vanadium, whereas the respective ground states for Nb and Ta are best described as closed-shell singlets. Unfortunately, no further details on how this change in spin state from the first-row to the 2nd and 3rd row congener relate to potential reactivity of these complexes are available to date.

The metal-catalyzed transfer of oxygen atoms is of great importance for both industry and nature. This reaction classically involves the transfer of an O atom from a high-valent metal center onto a substrate accompanied by a formal two electron reduction of the metal.³⁶ Subsequently, the metal-oxo is regenerated by an oxidant accompanied by a formal two-electron oxidation of the metal center. The group of Brown showed that this reaction can also take place in a nonclassical way by employing redox-active catecholates ligands.³⁷ Air- and moisture stable complex **29** was readily synthesized by a reaction of two equivalents of 3,5-di-*tert*-butyl-catechol with MoO₂(acac)₂ in the presence of pyridine-N-oxide. Although in solution multiple stereoisomers which readily interconvert were observed, only one stereoisomer was observed in the solid state. Complex **29** was found to be stable for extended periods at room temperature. However, upon heating to 70 °C in the presence of excess pyridine-N-oxide the complex was converted into 3,5-di-*tert*-butyl-1,2-benzoquinone, pyridine and MoO₃•Opy (Scheme 15). Mechanistic investigations (kinetics, substituent effects and activation parameters) indicate that the rate limiting step in the pyridine deoxygenation is the expulsion of pyridine from complex **29** forming proposed intermediate **30**. In this nonclassical oxygen atom transfer reaction, the electrons required for pyridine deoxygenation are drawn from the catecholates ligands prior to their dissociation as quinone, not changing the formal oxidation state of Mo. Unfortunately, the group was unable to produce a stabilized analogue of intermediate **30**. More recently the group reported a seven-coordinated analogue of complex **29** bearing an additional redox-active catecholate in the red²⁺ oxidation state instead of the oxo moiety.³⁸ This complex also reacts upon heating in the presence of excess pyridine-N-oxide to initially form **29** and ultimately MoO₃•Opy, pyridine and 3,5-di-*tert*-butyl-1,2-benzoquinone. Notably, the decay of the new complex shows an autocatalytic profile due to a rapid comproportionation with **29**. Although the mechanism to form **29** from this complex was not investigated in such great detail as for the example shown in Scheme 15, the authors propose that it follows an analogous mechanism involving a nonclassical oxygen atom transfer.



Scheme 15 Nonclassical oxygen atom transfer from a coordinated pyridine-N-oxide to a Mo complex.

The group also reported an example of a nonclassical oxygen atom transfer in the synthesis of oxorhenium complex **32** (Scheme 16).³⁹ A reaction of previously reported transmetalation agent **31**,⁴⁰ containing two redox-active ONO ligands in the **q** oxidation state, with $\text{ReO}_2(\text{PPh}_3)_2$ forming PbI_2 , OPPh_3 and complex **32**. Interestingly, the redox-active ligand is reduced by two electrons to the **red**²⁻ oxidation state in the reaction. The electrons required for this reduction are supplied by the oxidation of PPh_3 to OPPh_3 in a nonclassical oxygen atom transfer. Characterization by multinuclear NMR spectroscopy, UV-vis spectroscopy and X-ray crystallography confirmed the **red**²⁻ oxidation state of the ONO ligand. The authors mention that although the overall transformation is a nonclassical oxygen atom transfer, it is not clear whether the mechanism is nonclassical in this case.



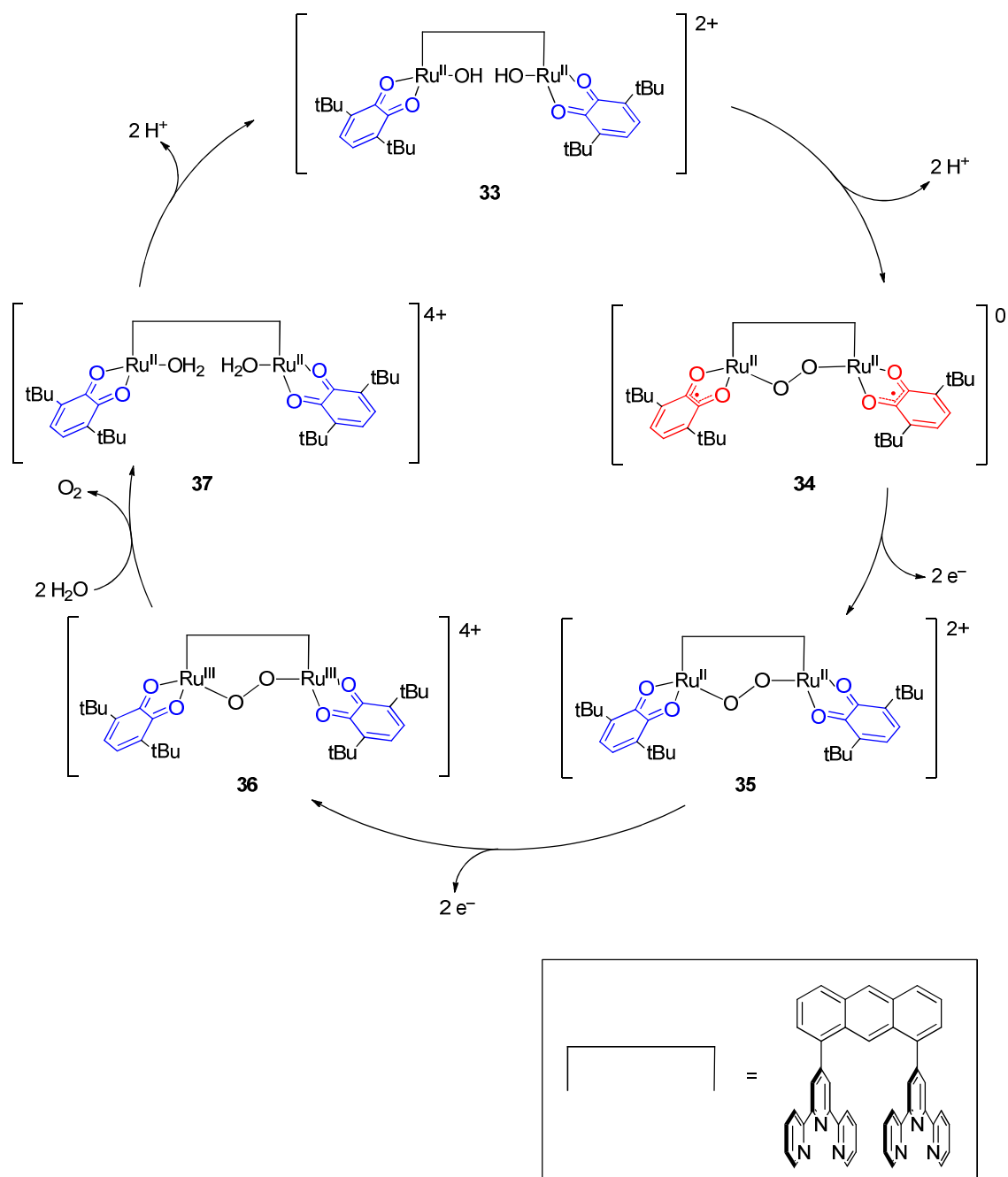
Scheme 16 Nonclassical oxygen atom transfer in the synthesis of complex **32**.

b) Late Transition metals

Late transition metals, especially the 2nd and 3rd row elements, have a well-established role in catalysis due to their ease of two-electron oxidation state changes. Many catalytic processes include elementary steps such as oxidative addition or reductive elimination, which proceed via two-electron steps and require accessible M^{n+} and $\text{M}^{(n+2)+}$ oxidation states. The first-row (base) metals do not necessarily allow the same transformations and often preferentially undergo single-electron changes (*e.g.* Fe(II)/Fe(III) couple). The combined action of a redox-active ligand and a base metal may allow to mimic the prolific chemistry exhibited by noble metals in two-electron transfer processes without the requirement to access high-energy redox-states. Alternatively, 2nd and 3rd row-transition metals in high oxidation states may lack redox-equivalents that can be compensated for by the presence of a redox-active ligand. The Wieghardt group has contributed significantly to elucidate the coordination chemistry and to describe the electronic structure of redox-active catechol, *o*-aminophenol and *o*-phenylenediamine ligands with late transition metals.⁴¹ This work has been essential to our understanding on how these ligands can bind and react in different oxidation states to metals.

The application of redox-active quinone-containing ligands for Ru-mediated water oxidation catalysis was reported by Tanaka. The catalyst consists of two terpyridine fragments anchored to a dinucleating rigid anthracene scaffold amenable to hosting two ruthenium metal centers, with one redox-active quinone ligand as well as a hydroxy fragment per Ru (**33**, Scheme 17).⁴² The mechanism of water

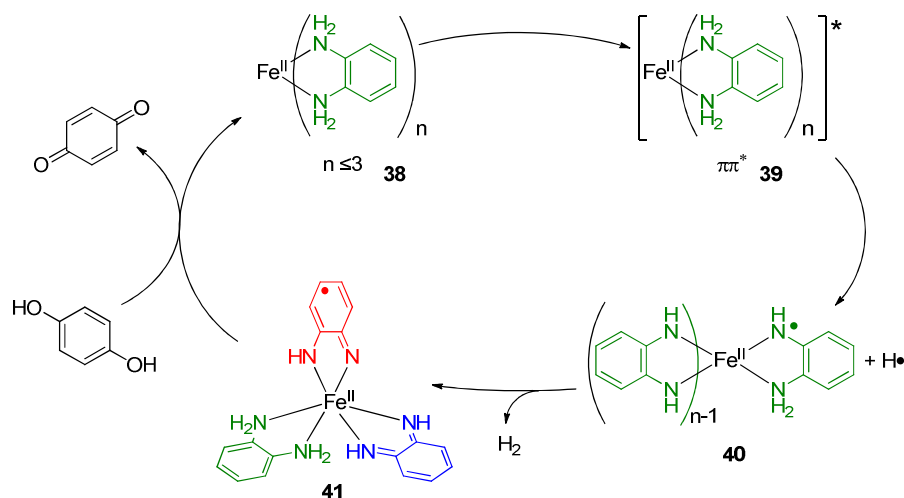
oxidation using this catalyst has been subject to extensive research in the following years, both experimentally and theoretically.⁴³ Cyclic voltammetry studies indicated a ligand-localized oxidation at $E_{1/2} + 0.40$ V (vs Ag/AgCl) and a metal-localized oxidation of $[\text{Ru}^{\text{II}}_2(\text{O})_2(3,6\text{-tBu}_2\text{qui})_2(\text{btpyan})]^{2+}$ at +1.2 V. Controlled-potential electrolysis of $[\text{1}](\text{SbF}_6)_2$ at a potential of +1.70 V in the presence of H_2O in $\text{CF}_3\text{CH}_2\text{OH}$ resulted in dioxygen evolution with a current efficiency of 91% (21 turnovers). The proposed electrocatalytic cycle for this four-electron process is depicted in Scheme 14. Interestingly, the ruthenium metal centers mostly remain in the Ru^{II} oxidation state, while the quinone ligands facilitate the redox chemistry throughout the process. Deprotonation of **33** results in formation of bridged peroxy-complex **34**, which is facilitated by reduction of the quinone ligands from the **q** to the **sq⁻** oxidation state. It was found that the quinone ligands are indeed required for catalytic turnover in the proposed pathway. An analogous complex with bipyridine ligands instead of quinones resisted deprotonation, even when excess of KO^tBu was added, preventing the essential O-O bond formation. Subsequent four-electron oxidation via intermediates **35** results in the formation of complex **36** and involves oxidation of both the ruthenium centers (from Ru(II) to Ru(III)) and the OO-ligands (from **sq⁻** to **q**). Reaction with two molecules of H_2O leads to release of O_2 and complex **37**, which can undergo double deprotonation to regenerate **33**.



Scheme 17 Proposed mechanism for catalytic water oxidation using dinuclear Ru(quinone) complex by Tanaka.

The application of redox-active ligands for photochemical hydrogen evolution at room temperature was reported by Kato and Chang *et al.*, using a dicationic tris(*o*-phenylenediamine) iron(II) complex (Scheme 18).⁴⁴ Preliminary mechanistic investigations suggest that (at least) one of the *o*-phenylenediamine ligands of complex **38** is excited upon UV-irradiation at ~ 298 nm (via species **39**), resulting in N-H bond homolysis to give an H-atom and an *o*-aminoanilino radical (**40**). A second H-

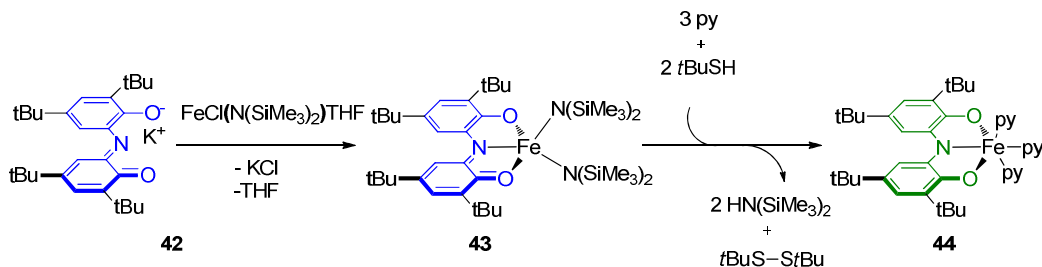
atom abstraction from the ligand may generate H_2 . This also produces an iron complex with either one two-electron oxidized or two one-electron oxidized ligands, which can undergo reduction by external hydroquinone, functioning as both electron- and proton-donor. An exciting possibility would be to tune the electronic properties of the ligands in such a fashion that the reaction could also be performed with visible light for H_2 storage applications.



Scheme 18 Proposed mechanism for the photochemical hydrogen evolution reaction of hydroquinone with a dicationic tris(*o*-phenylenediamine) Fe(II) complex.

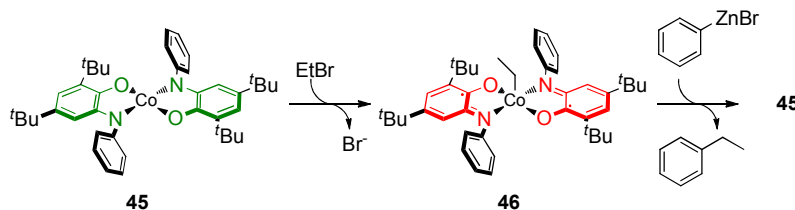
The group of Heyduk recently showed that reductive elimination of disulfides from an Fe(III) complex could be performed without changes in metal oxidation state by using a redox-active ONO ligand (Scheme 19).⁴⁵ Interestingly, the only way to avoid the formation of homoleptic $\text{Fe}(\text{ONO})_2$ complexes was to first oxidize the ONO ligand to the **q** oxidation state. Reacting the potassium salt of the ONO^{q} ligand (**42**) with $\text{FeCl}(\text{N}(\text{SiMe}_3)_2)(\text{THF})$ resulted in the formation of complex **43**. The crystal structure obtained for this species displays alternating C-C and C=C bond lengths for the ligand backbone as well as two C=O bonds, which is in agreement with the **q** oxidation state being retained upon coordination to iron. EPR and Mössbauer spectroscopy showed the complex to be a high-spin $S = 5/2$ iron(III) species. Reaction of complex **43** with *tert*-butylthiol in the presence of three equiv pyridine) resulted in the formation of di-*tert*-butyldisulfide and the formation of complex **44** featuring a two-electron reduced ligand. These observations suggest that the $\text{Fe}(\text{ONO})$ platform can promote reductive elimination of disulfide without changing the *metal* oxidation state. The authors were unable to isolate or observe the disulfide intermediate. Three possible mechanisms were proposed regarding the disulfide formation: i) a thiol-thiolate coupling, ii) a bimetallic pathway and iii) ligand-assisted reductive elimination. Mechanistic investigations, which are lacking to date, could

aid to further expand the design of catalyst systems using an abundant metal such as iron in combination with redox-active ligands.



Scheme 19 Redox-active ligand facilitated reductive elimination of a disulfide from Fe(III).

In 2010, Soper *et al.* reported a square planar cobalt(III) complex able to catalyze a Negishi-like cross-coupling of alkyl halides with organozinc reagents (Scheme 20).⁴⁶ The starting Co^{III} complex (**45**) has two coordinated amidophenolato ligands in the red^{2-} oxidation state. Because cobalt is a first-row transition metal, it is mostly associated with single-electron radical reactions. However, complex **45** reacts as a nucleophile toward an alkylhalide, quantitatively affording the square pyramidal ethyl complex **46**. The electrons needed for this oxidative addition are provided by the two NO ligands, which are both oxidized to the sq^- oxidation state. Upon treatment of complex **46** with organozinc bromide compounds, *e.g.* PhZnBr , complex **45** is regenerated and C–C bond-formation is observed. Although these stoichiometric reactions constitute a hypothetical catalytic cycle, data on the application of **41** as catalyst for cross-coupling is not reported to date.

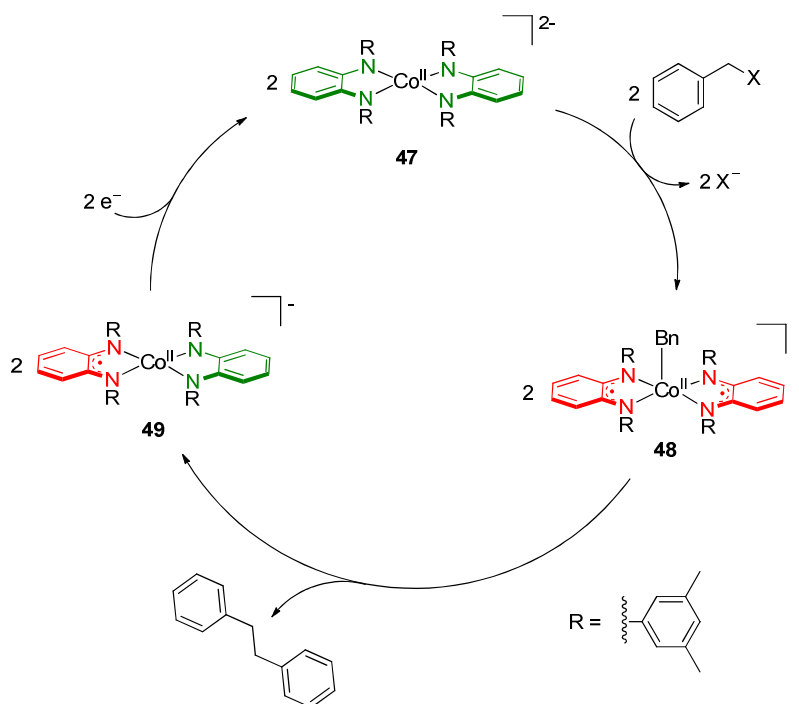


Scheme 20 Negishi-like cross-coupling of alkyl halides with organozinc reagents by a bis-amidophenolato Co(III) complex.

Group 10 metals (Ni, Pd) are commonly applied for cross-coupling reactions, as they relatively easily facilitate two-electron transfer by virtue of $\text{M}^0\text{--M}^{\text{II}}$ redox cycles. Cobalt is a less obvious choice for this type of chemistry, but a combination of metal and ligand based redox *or* even a ligand-only strategy to enable two-electron transfer could provide entry into such cross-coupling chemistry.

Recently, Sarkar *et al.* reported a four-coordinate cobalt species capable of electrocatalytic C–C bond formation (Scheme 21).⁴⁷ The cobalt(II) center has two *o*-phenylenediamide-derived ligands coordinated in their sq^- oxidation state. Cyclic voltammetry showed two fully reversible one-electron reduction waves in THF ($E_{1/2} = -1.23$ V and -2.10 V vs Fc/Fc^+), while the CV in CH_2Cl_2 showed the onset of a catalytic current at the potential for the second reduction (onset at -2.1 V vs Fc/Fc^+). This

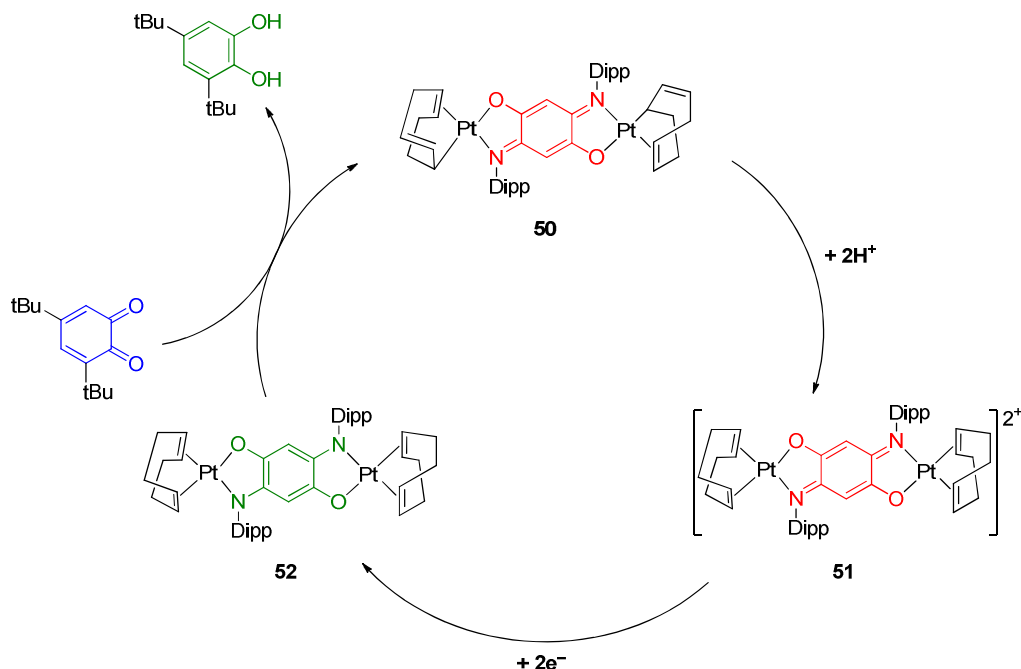
stimulated investigations into the electrocatalytic activation of carbon-halogen bonds, with the conversion of benzyl bromide into dibenzyl chosen as proof-of-principle. The addition of two equivalents of benzyl bromide to *in situ* generated complex **47** resulted in the isolation of dibenzyl. The proposed mechanism starts with nucleophilic attack of complex **47** on benzyl bromide, accommodated by ligand oxidation to the sq^- oxidation state to form **48**, analogous to the work of Soper (Scheme 18). The authors do not speculate on possible pathways for the actual C-C bond forming step. A bimolecular process could be envisioned, resulting in ligand mixed-valent species **49** which may undergo reduction to regenerate complex **47**.



Scheme 21 Electrocatalytic coupling of dibenzyl by a bis-phenylenediamine Co(II) complex.

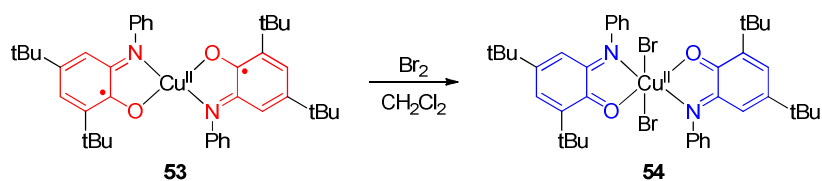
Sarkar also recently reported a dinuclear platinum complex that is able to donate two protons and two electrons. This system is constructed from redox-active 2,5-di-[2,6-(diisopropyl)anilino]-1,4-benzoquinone as dinucleating ligand, and with two C(allyl)-H activated 1,5-cyclooctadiene (cod) fragments to complete the square planar geometries around the two Pt(II) centers (species **50**). The benzoquinone-based ligand acts as an electron reservoir, while the activated 'diene' is postulated to serve as proton-reservoir (Scheme 22; the η^1 -coordination mode for the alkyl-alkene ligand is shown). Protonation of the Pt-C_{allyl} fragment generates **51** with two neutral cod ligands. Two-electron reduction using exogenous reductant (CoCp₂) transforms the redox-active quinoid bridge into the amidophenolato red^{2-} form (complex **52**). Both processes were found to be reversible under judicious reaction conditions. Furthermore, 3,5-di-*tert*-butyl-benzoquinone can be applied as both proton and

electron acceptor, yielding the catechol derivative, which regenerates **50**. Also in this case, the hypothetical catalytic cycle is composed of individual stoichiometric steps to date.



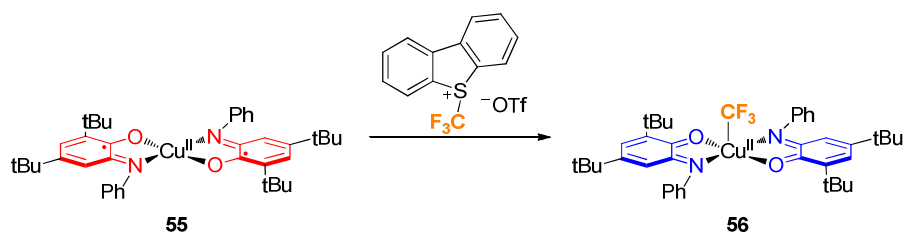
Scheme 22 Bimetallic platinum complex as a two proton and two electron donor in the stoichiometric reaction with 3,5-di-*tert*-butylquinone.

Chaudhuri *et al.* reported the ligand-assisted oxidative addition of molecular bromine to a copper(II) complex containing two redox-active amidophenolato ligands (**53**, Scheme 23).⁴⁸ The reaction is similar to those reported by Heyduk (*vide supra*) with Zr in the sense that Cu retains its formal (+II) oxidation state and the two redox-active ligands are each oxidized by one electron. However, the ligands are oxidized from the sq^- to the q oxidation state (rather than red^{2-} to sq^- oxidation), obtaining a hexacoordinated Cu^{II} complex (**54**). This species was found to react with triethylamine to generate acetaldehyde and diethylamine in the presence of water. EPR spectroscopy of this reaction mixture indicated the presence of a ligand centered radical, which was explained by an overall two-electron reduction, with one ligand being reduced from q to sq^- and the second reduction occurring at Cu (Cu^{II} to Cu^{I}).



Scheme 23 Ligand assisted oxidative addition to a Cu(II) complex.

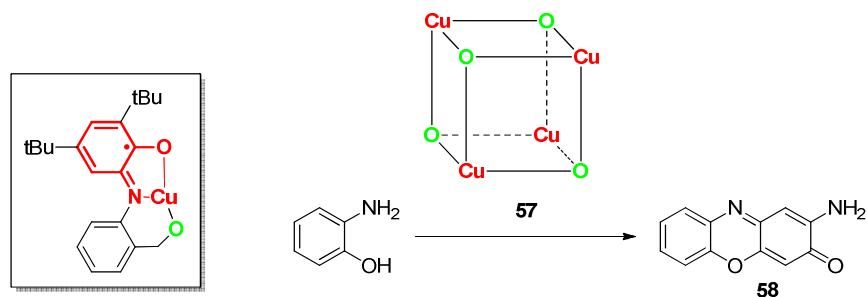
Fensterbank *et al.* recently reported new reactivity with the same copper(II) complex.⁴⁹ Introduction of a trifluoromethyl group was achieved by reacting complex **55** with the Umemoto reagent⁵⁰ at room temperature and under inert atmosphere, providing five-coordinate Cu^{II} species **56** (Scheme 24). Formal oxidative addition of the electrophilic CF₃⁺ group leads to one-electron ligand oxidation (from **sq**⁻ to **q**) whilst retaining the copper(II) oxidation state. The resulting Cu(CF₃) complex promotes trifluoromethylation at available electrophilic sites (the C-O and C-N units) within the coordinated ligand. This observation suggests a formal *umpolung* of the CF₃ moiety. Trifluoromethylation of external partners was unsuccessful to date. However, addition of the N-tolyl analogue of the ON ligand to complex led to trifluoromethylation of this exogenous substrate, which indicates that ligand exchange is required for this reactivity to occur.



Scheme 24 Reaction of complex **55** with Umemoto's reagent, performing a formal *umpolung* for CF₃.

In 2007 Chaudhuri *et al.* reported a cubic tetranuclear copper(II) species **57** bearing four ligand-centered radicals. This complex was applied as a functional model of the enzyme phenoxazinone synthase (Scheme 25).⁵¹ The cubic structure is constructed from four copper(II) ions and four tridentate amidophenolato-type ligands (with a pendant alkoxide donor) in the **sq**⁻ oxidation state. Variable temperature magnetic susceptibility (SQUID) measurements of the complex, which contains eight paramagnetic centers (four ligands, four copper ions), established a diamagnetic ground state ($S = 0$) due to antiferromagnetic interactions. Electrochemical measurements and UV-Vis spectroscopy showed that the first four reduction processes are primarily ligand-centered, followed by two metal-centered reductions. Besides having a fascinating structure, complex **57** was found to be able to catalytically oxidize 2-aminophenol to 2-aminophenoxazine-3-one (**58**), under aerobic conditions, thus modelling the enzyme phenoxazinone synthase. Under anaerobic conditions only one turnover was achieved, which established the necessity for aerial oxidation. A tentative catalytic cycle

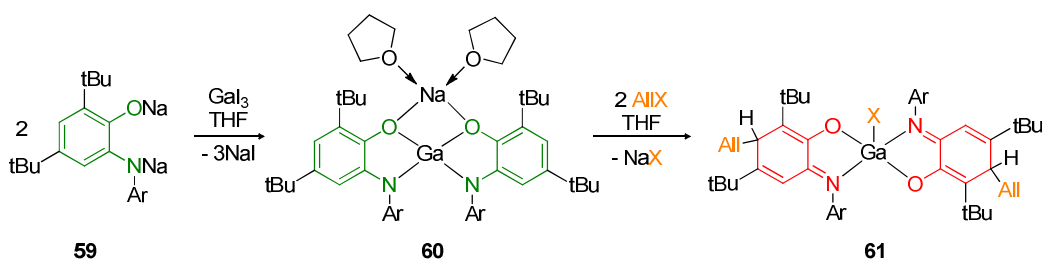
involving a complex interplay between ligand- and metal-centered redox processes was proposed on the basis of kinetic and electrochemical data but the authors correctly state that several mechanisms may be operational for this complex reaction.



Scheme 25 Schematic representations of the tetracopper(II) tetraradical complex and its ability to catalyze the oxidation of *o*-aminophenol to 2-aminophenoxazine-3-one.

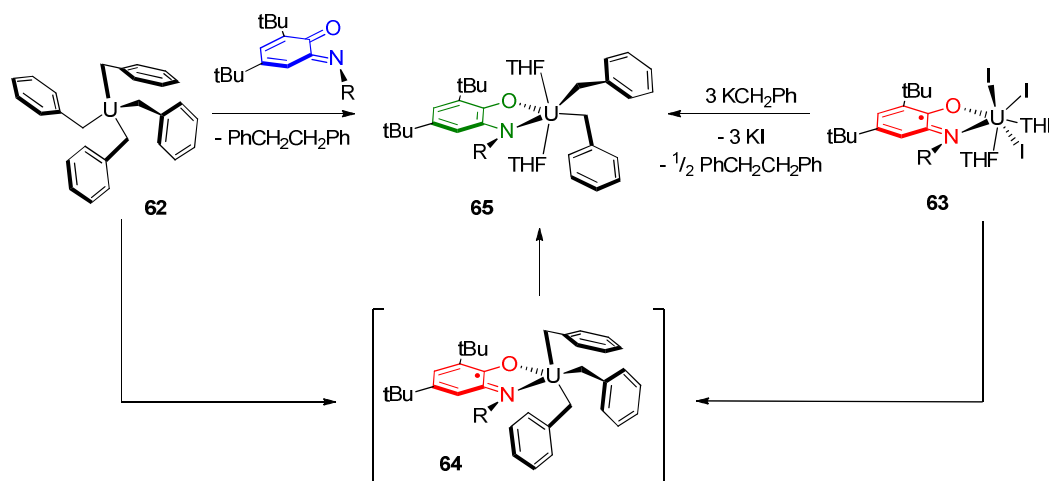
c) Other metals

The ability to use redox-active ligands as a strategy to expand reactivity is not limited to transition metals. A recent example by Piskunov *et al.* demonstrates unusual reactivity with a gallium(III) complex containing two *o*-amidophenolate-based ligands (**59**, Scheme 26).⁵² The reaction of GaI₃ with the disodium salt of the substituted *o*-aminophenol yields an interesting complex containing both sodium and gallium in distorted tetrahedral geometries (**60**). X-ray diffraction shows that the sodium is coordinated to the oxygen atoms of the amidophenolate ligands, as well as to two solvent molecules (THF). This heterometallic compound reacts with two equivalents of an allyl halide to give **61**, wherein C-C bond formation (allylation) has occurred at the amidophenolate backbone. This reaction readily proceeds at room temperature and shows that the steric *tert*-butyl groups are not always sufficient to protect the redox-active ligand. The same group previously reported comparable reactivity with a related indium(III) complex,⁵³ although the reaction was performed with alkyl halides and required elevated temperatures to proceed.



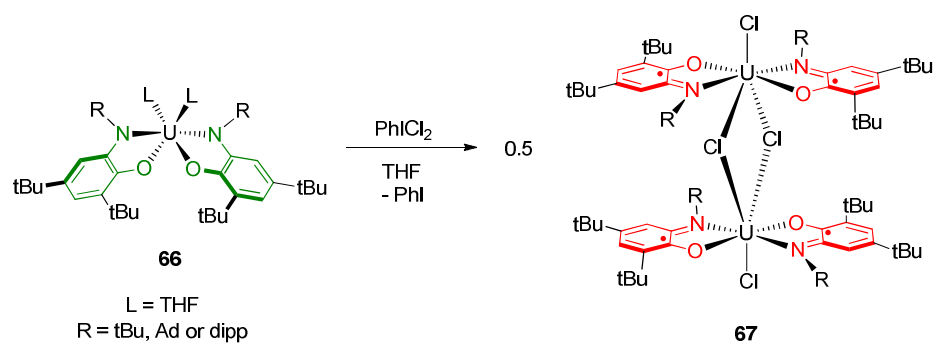
Scheme 26 Synthesis and addition of allyl halide on a gallium(III) complex.

Recently, Bart *et al.* reported uranium(IV)tetrabenzyl complex (**62**) that can undergo radical reductive elimination of 1,2-diphenylethane, mediated by an iminoquinone-based (**q**) ligand in a process that avoids the intermediacy of unstable divalent uranium species.⁵⁴ A crossover experiment with the fully deuterated tetra(benzyl)uranium analog indicates that the mechanism proceeds via stepwise benzyl radical extrusion, presumably involving intermediate **64** and with finally formation of species **65** and one equivalent of PhCH₂CH₂Ph (Scheme 27). This complex contains the redox-active ligand in the **red**²⁻ oxidation state. Attempts to isolate intermediate **64** by reaction of U(IV) complex **63**, with the redox-active iminosemiquinone ligand (**sq**⁻) already installed, with benzylpotassium also resulted in the formation of **65** and PhCH₂CH₂Ph.



Scheme 27 Two synthetic routes for the synthesis of **65** and possible intermediate for the radical reductive elimination. R = 2,6-diisopropylphenyl.

Bart *et al.* also reported how redox-active amidophenolate ligands can facilitate oxidative addition on a uranium(IV) complex (Scheme 28).⁵⁵ Inspired by the ligand-facilitated oxidative addition to d^0 metals reported by Heyduk, the group added PhICl₂ to complex **66** bearing two NO (**red**²⁻) ligands, resulting in the formation of dinuclear uranium complex **67**, featuring two bridging chlorido ligands. Both uranium centers are still in the (+IV) oxidation state but the four redox-active ligands are oxidized from the **red**²⁻ to the **sq**⁻ oxidation state. Using the *tert*-butyl substituted amidophenolate derivative, oxidative addition of I₂ was facilitated to yield a mononuclear analogue of **67**, whereas with other *N*-substituents this reaction with iodine resulted in decomposition.



Scheme 28 Oxidative addition of Cl_2 from PhICl_2 onto bis(*o*-aminophenolate) U(IV) complex **66** forming complex **67**.

3) Beyond Electron reservoirs

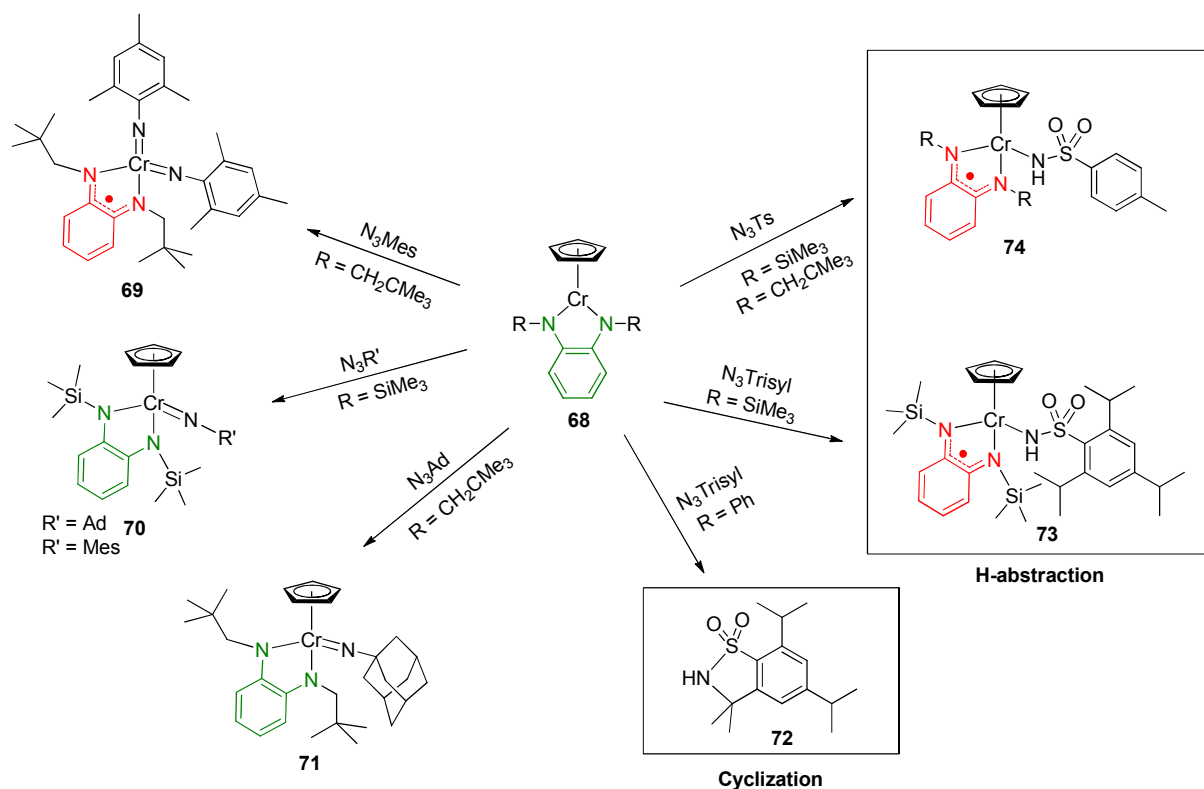
Although the major use of redox-active ligands to date is to act as one- or two-electron reservoir for reactivity at a metal center, these reactive organic frameworks exhibit additional unique properties of relevance for stoichiometric and catalytic applications. A prime example that is generating much attention lately is the ability to stabilize or generate substrate-centered radicals in the coordination sphere of a (transition) metal. This enables controlled odd-electron (radical-type) reactivity upon metals commonly not disposed for one-electron redox-chemistry (e.g. most noble metals). This new avenue in the field of redox-active ligand-assisted chemistry demonstrates that scientists have yet to discover its full potential. The ability to change the Lewis-acidity or -basicity of a metal center by changing the ligand oxidation state is another example how redox-active ligands can enlarge the reactivity window relevant to the field of redox-switchable catalysis. Moreover, redox-active ligands can also show cooperative behavior, meaning that these entities may show chemoresponsive behavior and actively partake in bond-making and bond-breaking processes.

a) Production of substrate-centered radicals

Fine-tuning of the orbital energies within a complex makes it possible to stabilize ligand-centered radicals by delocalization over the organic framework. Additionally, the same fine-tuning can allow, upon a suitable stimulus, for intramolecular single-electron transfer from a redox-active ligand to a metal-bound substrate, thereby generating a substrate-centered radical.

An elegant example demonstrating the subtleties associated with this fine-tuning was recently reported by Smith *et al.*, regarding the effect of redox-active *o*-phenylenediamido ligands on hydrogen-abstraction reactivity of chromium(imido) species (Scheme 29).⁵⁶ The activation of organoazides on Cr(Cp)(NN) complexes bearing differently substituted *o*-phenylenediamine (NN) frameworks (**68**) was investigated. Using mesitylazide and neopentyl-substituents on the redox-active ligand, the corresponding formally Cr(V)-based bis(imido) species **69** was obtained, with one-electron oxidation of the NN ligand. In some cases, the expected chromium(imido) complex was obtained (**70**, **71**) with no change in ligand oxidation state (red^{2-}) and the Cp-ring still coordinated. Interestingly, for some N-based substituents, an additional H-atom abstraction reaction (likely from solvent, although a bimolecular hydrogen-atom transfer mechanism is another option) took place, accompanied by single-electron oxidation (red^{2-} to $\text{sq}^{\cdot-}$) of the redox-active ligand (**73** and **74**). Moreover, the phenyl-substituted *o*-phenylenediamine ligand resulted in a catalytically active complex for the formation of benzosultam **72** by an intramolecular C-H activation and cyclization, albeit with a TON < 5. This reactivity can be explained by single-electron transfer from the redox-active ligand to the imido substrate to form a reactive imido nitrogen-centered (imidyl or nitrene) radical. Subsequent intramolecular hydrogen atom abstraction followed by a radical rebound or direct C-H insertion

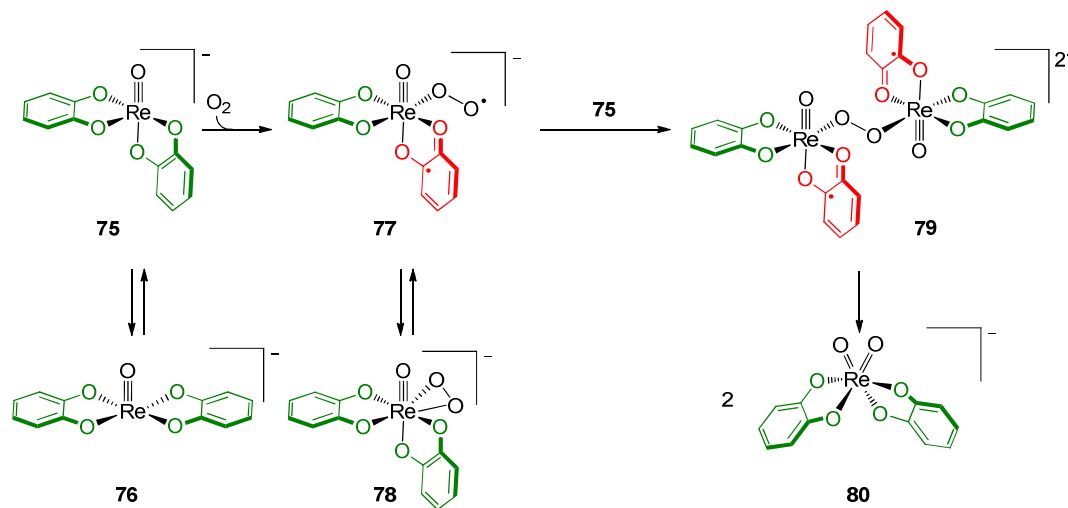
generates the benzosultam. For the complexes that displayed stoichiometric reactivity the magnetic moment was determined (using Evans' method) as well as the solid state structure (from X-ray crystallography). The isolation of a Cr^{III} complex with a monoanionic **sq**⁻ ligand radical lends support to an intramolecular redox-active ligand-to-substrate single-electron transfer mechanism. DFT calculations could shed more light on this proposed pathway.



Scheme 29 Reactions of *o*-phenylenediamine-derived chromium(III) complex reactions with different azides.

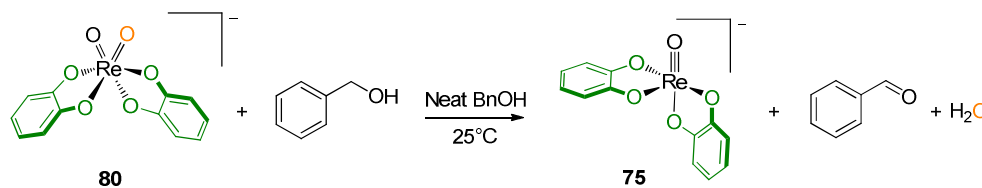
In 2010, Soper and co-workers reported the bimetallic O₂ homolysis at five-coordinate oxorhenium(V) complexes facilitated by a redox-active ligand (Scheme 30).⁵⁷ Even though the splitting of O₂ with second or third-row transition metals is not very rare,⁵⁸ most of the oxygen-atom acceptors are unreactive toward dioxygen. Soper and co-workers synthesized two new oxorhenium(V) complexes containing either two 2,4-di-*tert*-6-(phenylamido)phenolate ligands or two catecholate ligands (shown in Scheme 28 as species **75**). The redox-active ligands proved to be crucial to enable O₂ homolysis, acting as electron reservoir. A structural homologue with redox-inert oxalate ligands did not show any reactivity toward O₂, strongly indicative of active involvement of the redox-active ligands. A combination of kinetic experiments and computational resulted in the proposed mechanism

depicted in Scheme 30. Coordination of O_2 to rhenium, to form the rhenium($O_2^{\cdot -}$) intermediate **77** bearing a superoxide fragment, formally requires one-electron oxidation at rhenium, but the rhenium(VI) oxidation state which is very rare.⁵⁹ By using the redox-active ligand as a single-electron donor in this process this unusual scenario is circumvented, which significantly lowers the activation barrier. Hence, one of the catecholato or 2-aminophenolato dianion frameworks undergoes oxidation to the $sq^{\cdot -}$ oxidation state, creating a ligand mixed-valent complex. Furthermore, delocalization of spin density onto the ligand may lower the barrier for spin-crossover for the formally spin-forbidden reaction of the rhenium(V) complex with O_2 . This second role of the ligand is likely also relevant to facilitate attack of the superoxo radical onto a second rhenium(V) complex to form the peroxo-bridged complex **79**. This dinuclear species can split into two oxorhenium(V) complexes (**80**). Overall the reaction adds one oxygen atom to the rhenium complex (oxygenation), oxidizing the rhenium(V) to rhenium(VII), facilitated by the redox-active ligands. The proposed mechanism for the catecholato complex shown in Scheme 30 is assumed to also be operational for the bis-aminophenolato complex. The same group reported deoxygenation of the stable nitroxyl TEMPO \cdot radical via homolytic N-O bond splitting using the same strategy.⁶⁰



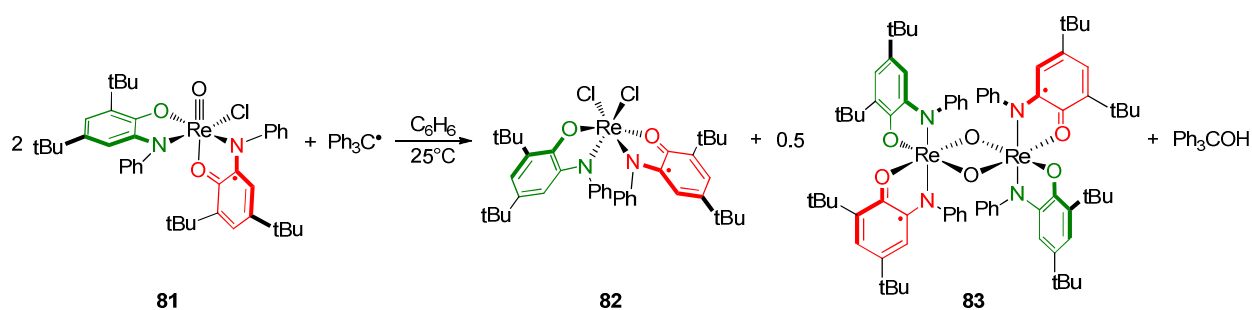
Scheme 30 Proposed mechanism for the bimetallic O_2 cleavage by oxorhenium(V) complexes.

Soper and coworkers also reported on an application for complex **80** to oxidize benzyl alcohol under aerobic conditions.⁶¹ Complex **80** reacts with benzyl alcohol to regenerate dioxorhenium(VII) complex **75** (Scheme 31) as well as benzaldehyde and water, which is formed from the net abstraction of H_2 from benzyl alcohol. Although the catalytic performance (TON of 7) is poor, this example illustrates the potential for implementation of redox-active ligands in catalysis.



Scheme 31 Oxidation of benzylalcohol by bis-catechol dioxorhenium(VII).

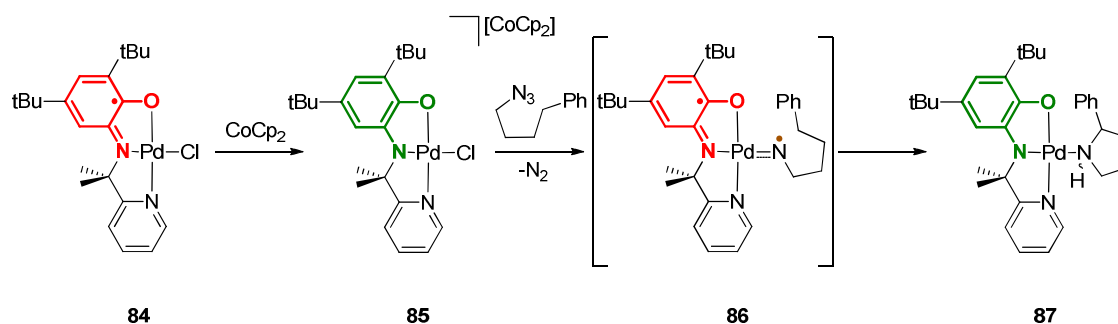
The group of Soper envisioned that having a redox-active ligand on a coordinatively *saturated* metal center would induce redox reactions at a ligand (assuming the role of coordinated substrate), rather than simply supplying electrons for a coordinatively *unsaturated* metal center. The coordinative saturated Re complex **81** is generated by reaction of the Re(V)-oxo precursor with a Cl^+ donor to add chlorine *cis* to the oxo ligand (Scheme 32).⁶² To determine if the redox-active ligand could induce redox activity onto another ligand, complex **81** was reacted with a source of triphenylmethyl radical ($\text{Ph}_3\text{C}^\bullet$). The main organic product was found to be triphenylmethanol (Ph_3COH), and two new rhenium complexes – dichlorido-species **82** and oxo-bridged dimer (**83**) were also detected. The authors propose that mixing of a populated $\text{Re}=\text{O}$ π -bond with the ligand-centered sq^\bullet radical leads to substantial oxyl radical character (O^\bullet) for the oxo fragment, which enables the low-barrier radical coupling. Upon one-electron reduction of **77** and subsequent reaction with Ph_3C^+ , the latter acts as a single-electron oxidant to produce the dimer **83** without formation of Ph_3COH . Rhenium complex **83** is likely the result of an oxygen-atom transfer. Although this reaction does not necessarily confirm the unpaired spin density at the proposed oxyl fragment by redox-active ligand-to-substrate transfer, closed-shell oxorhenium homologues were found to be inert to $\text{Ph}_3\text{C}^\bullet$. Computational studies could shed more light on this reactivity and potentially elucidate the subtle role of the electronic structure of the donor set in this Re-chemistry.



Scheme 32 Reaction of complex **77** with $\text{Ph}_3\text{C}^\bullet$, yielding Ph_3COH and two rhenium complexes **82** and **83**.

Recently, our own group reported the first example wherein a redox-active ligand conveys odd-electron (radical-type) reactivity onto a noble metal (Pd) that is typically not disposed for single-electron transformations.⁶³ Coordination of the redox-active tridentate aminophenol-based NNO ligand to a palladium(II) precursor afforded the square planar paramagnetic complex **84** with a closed-

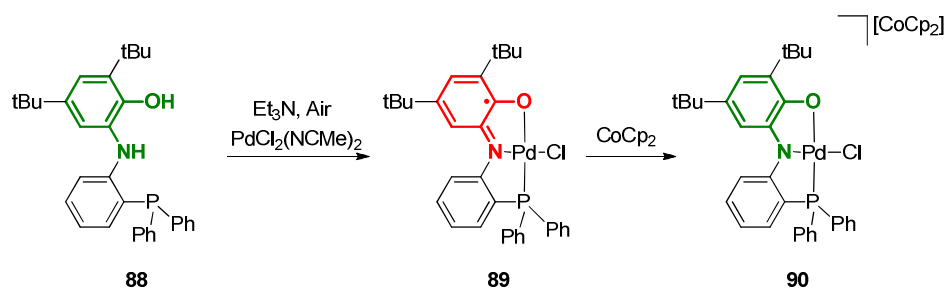
shell Pd^{II} ion and a ligand-centered radical (Scheme 33).⁶⁴ DFT calculations, EPR spectroscopy and single crystal X-ray diffraction confirmed the **sq⁻** oxidation state of the ligand. Cyclic voltammetry showed fully reversible one-electron oxidation ($E_{1/2} = +0.04$ V) and reduction events ($E_{1/2} = -1.11$ V vs. Fc/Fc⁺), that are proposed to be fully ligand-based. Chemical reduction with CoCp₂ afforded diamagnetic analogue **85** wherein the NNO ligand is reduced to the **red²⁻** oxidation state. DFT calculations suggested that replacement of the chloride ligand in **85** by a nitrene (imido) species could result in the generation of a nitrene radical upon intramolecular redox-active ligand-to-substrate single-electron transfer. It was experimentally demonstrated that complex **85** is capable of activating 1-(4-azidobutyl)benzene and that this result in selective intramolecular benzylic C–H amination to produce the corresponding pyrrolidine. DFT calculations, isotopic labeling, and trapping experiments support a process that involves initial substitution of the chlorido ligand in the anionically charged species **85** by organoazide, followed by thermal expulsion of N₂ and formation of a nitrene adduct. Facile intramolecular single-electron transfer from the redox-active ligand to this substrate generates intermediate **86**. H-atom abstraction and radical-rebound produce the N-heterocyclic product. The nitrene radical species **86** was computed for all three possible spin states (open-shell and closed-shell singlet as well as triplet) with the former being thermodynamically favored for the entire pathway. This type of odd-electron radical-like reactivity is unprecedented with palladium and more inherent to base metals that easily generate reactive substrate radicals upon via single-electron pathways.⁶⁵ The unique combination of radical-type reactivity with the well-known strong substrate-binding properties of closed-shell noble metal ions might allow for the development of new catalytic reactions.



Scheme 33 Reduction of complex **84** and its ability to generate a reactive substrate-centered radical.

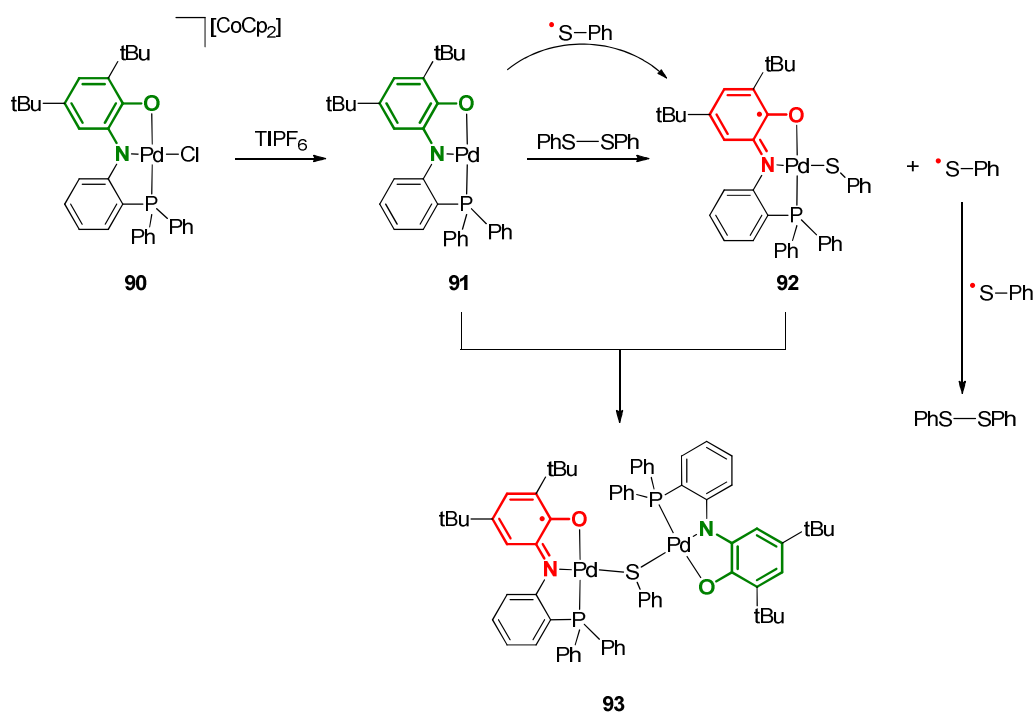
Following this work with Pd(NNO), a second example to showcase the potential for single-electron reactivity on palladium was recently published.⁶⁶ Herein, the first redox-active aminophenol-type ligand bearing a pendant phosphine was described (**88**, Scheme 34). Coordination of this PNO ligand to palladium(II) under aerobic and basic conditions afforded paramagnetic square planar complex **89** that shows resemblance to complex **84**. Thus, DFT, EPR and single crystal X-ray diffraction confirmed that the PNO ligand resides in the **sq⁻** oxidation state and spectroelectrochemistry showed that both the **q** and **red²⁻** oxidation states are easily accessible. However, the PNO ligand is less

electron-rich, with an $E_{1/2}$ of -0.75 V vs. Fc/Fc^+ , and thus more easily reduced than the corresponding pyridine-appended NNO system. One-electron reduction of **89** afforded diamagnetic complex **90** with the ligand in the red^{2-} oxidation state.



Scheme 34 Synthesis and single-electron reduction of complex **89**.

Treatment of this reduced complex with diphenyldisulfide in the presence of the halide abstracting agent TIPF_6 yielded dinuclear, paramagnetic palladium(μ -thiolate) complex **93**, with one PNO ligand per Pd. The monothiolate bridgehead is shown to arise from homolytic disulfide bond activation (Scheme 35). Use of bis(*tert*-butyl)disulfide allowed the detection of the neutral disulfide adduct. Notably the obtained crystal structure for **93** shows ligand-based mixed valence, with one PNO ligand in the red^{2-} and one in the sq^- state. Variable temperature EPR spectroscopy indicates that intramolecular electron transfer between these two electronically dissimilar ligands is facile in solution. Mechanistic investigations indicate that after chloride dissociation from the one-electron reduced species **90** and disulfide coordination, intramolecular ligand-to-disulfide single-electron transfer takes place to form $\text{PNO}^{\text{SQ}}\text{PdSPh}$ complex **92** and a thiyl radical. The thiyl radical can recombine to regenerate diphenyldisulfide, or react with a second equivalent of complex **91** to produce **92**. The strong tendency of sulfides to bridge two metal centers ultimately results in combination of **91** and **92** to give the dinuclear palladium species **93**. A 4:1 Pd:disulfide stoichiometry suffices for quantitative conversion. Cross-over experiments using a combination of diphenyldisulfide and ditolyldisulfide support in situ generation of thiyl species, as the mixed disulfide could be detected by GC-MS.



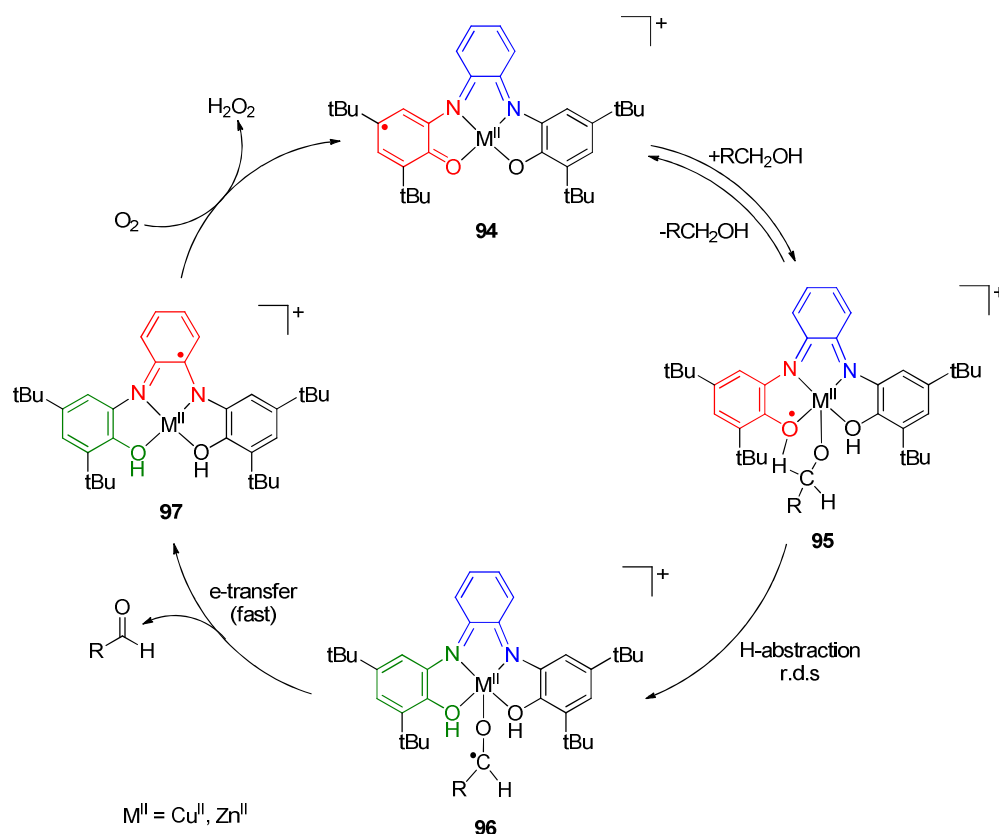
Scheme 35 Proposed mechanism for the formation of the μ -SPh bridged dinuclear Pd(II) complex **93**.

b) Ligand-centered cooperative reactivity

Bioinspired metal-ligand bifunctional activation of substrates and cooperative catalysis using ‘reactive ligands’ have attracted much attention in the last decade. A broad plethora of ligand motifs have been developed to facilitate a wide variety of bond activation processes.^{67,68} The redox-active ligands covered in this review can also actively partake in selective bond-making and bond-breaking processes via direct chemical interaction with substrates.

Wieghardt and co-workers reported the first examples of redox-active ligands acting as chemoresponsive frameworks for bond activation, using Cu^{II} and Zn^{II} complexes of a tetradentate redox-active ligand.⁶⁹ Inspired by the copper-containing metalloenzyme galactose oxidase, which catalyzes primary alcohols to aldehydes by means of a (thioether-modified) tyrosyl radical,⁷⁰ two catalyst systems were developed that could effectively oxidize primary alcohols with O_2 to aldehydes and H_2O_2 (Scheme 36). The ONNO ligand initially coordinated as the two-electron oxidized dianion to both metals, forming diamagnetic square planar species. Cyclic voltammetry showed two successive reversible single-electron oxidation steps (for Cu^{II} : -0.06 V and 0.41 V; for Zn^{II} : 0.03 V and 0.37 V vs. Fc/Fc^+) and also two successive reversible single-electron reduction steps (for Cu^{II} : -0.66 V and -1.42 V; for Zn^{II} : -0.64 V and -1.29 V vs Fc/Fc^+), indicating that five different ligand-

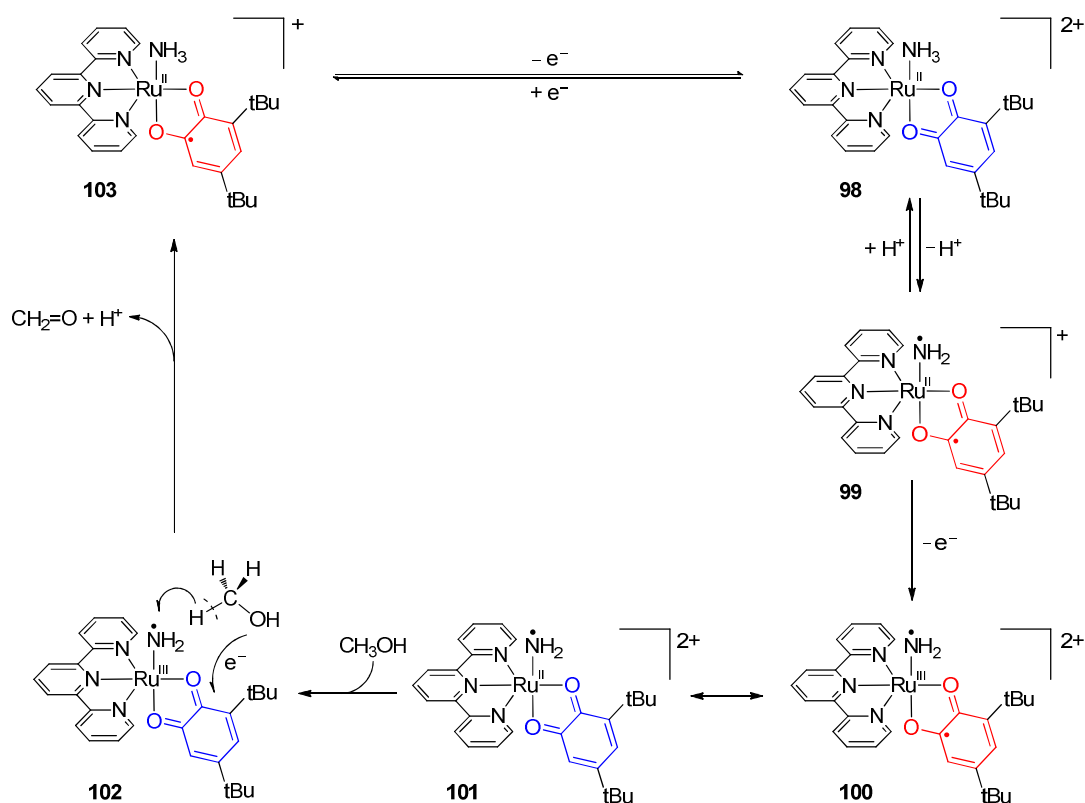
centered oxidation states are accessible for both complexes. It was found that under anaerobic conditions the one-electron oxidized species **94** oxidized primary alcohols in a stoichiometric fashion to afford the corresponding aldehydes and the single-electron reduced, doubly protonated complex **97**. In the presence of dioxygen, complex **94** is rapidly regenerated with concomitant formation of one equivalent of H_2O_2 , which closes the catalytic cycle. The reaction was performed with low catalyst loadings and ambient conditions. The copper complex showed superior reactivity ($\text{TOF} \sim 0.03 \text{ s}^{-1}$) over the Zn complex ($\text{TOF} = 0.002 \text{ s}^{-1}$) and reaching approx. 5000 turnovers within 50 hours. The initial (pre-equilibrium) step is proton-transfer from the alcohol to the phenoxide of the ONNO ligand with coordination of the generated alkoxide to the metal center to form **95**. Isotope labelling suggested that subsequent transfer of a β -hydrogen (H-atom abstraction) from the alkoxide by the quinone oxygen of the ONNO ligand to form **96** is the rate determining step in both cases.



Scheme 36 Proposed mechanism for catalytic oxidation of primary alcohols by dioxygen.

The group of Storr has reported well-characterized copper complexes bearing aminophenol derived redox-active ligands in various oxidation states and has shown that these complexes are also active catalysts for the aerobic oxidation of alcohols to aldehydes. However, no experimental evidence or proposal for the active role of the redox-active ligand in these transformation is provided.⁷¹ Tanaka and co-workers later reported a ruthenium-based system for the electrocatalytic oxidation of alcohols

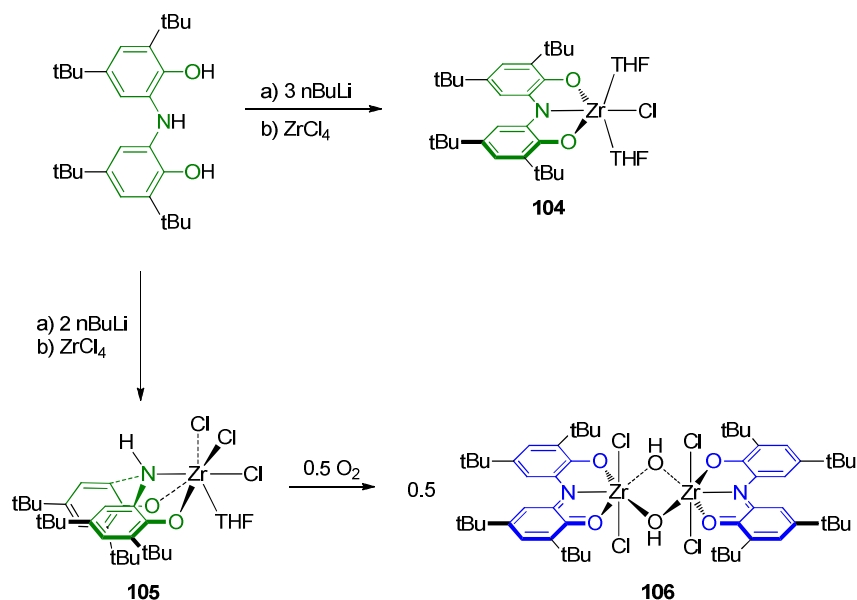
(methanol, ethanol and 2-propanol).⁷² The ruthenium precursor complex **98** contains a terpyridine, a redox-active quinone and a NH_3 ligand (Scheme 37). Upon deprotonation of this species in neutral water, the complex undergoes intramolecular electron transfer from the amide to the quinone ligand, yielding aminyl radical complex **99**. Subsequent one-electron oxidation results in either Ru^{III} diradical **100** or Ru^{II} monoradical **101**. The reaction with the alcohol likely proceeds via simultaneous H-atom abstraction by the aminyl radical and single-electron oxidation of quinone (**102**) to generate the oxidized analogue of the alcohol and **103**. The resulting complex can be oxidized by one electron to yield the starting compound. This pathway is based on earlier work describing the generation of such diradical-containing Ru^{II} complexes.⁷³ Recently reported DFT calculations, however, indicate that the H-atom abstraction step more likely occurs at complex **99**.⁷⁴



Scheme 37 Electrocatalytic oxidation of short-chain alcohols (methanol shown here) by a ruthenium catechol catalyst.

Heyduk *et al.* explored the use of an (phenol)aminophenol ONO ligand as both electron- and proton-reservoir for the reduction of molecular oxygen with zirconium(IV).⁷⁵ Similar to the Ta mentioned in section 2, the zirconium(IV) ion coordinates the triply deprotonated ONO trianion to form **104**. However, selective deprotonation of only the phenol-groups proved facile, as the pKa values for the O–H and N–H fragments are quite different. Reaction of the doubly deprotonated ligand with ZrCl_4 resulted in complex **105** (Scheme 38). The proposed structure shows a rather sterically hindered

conformation, but this proposal is only based on IR and NMR spectroscopic data. Nonetheless, complex **105** showed interesting reactivity towards O₂. Oxygen reduction to water is a complicated four-electron process.⁷⁶ Upon exposure to O₂, dinuclear complex **106** was isolated, wherein the O₂ is reduced to hydroxides that act as bridging ligands between the zirconium(IV) atoms. Both ONO ligands are present in the fully oxidized **q** oxidation state, which indicates that the ligand has provided two electrons as well as one (-NH) proton. The ligand oxidation state was confirmed by analysis of the bond lengths obtained from single crystal X-ray diffraction and by UV-vis spectroscopy. No mechanism for the formation of complex **106** has been proposed.



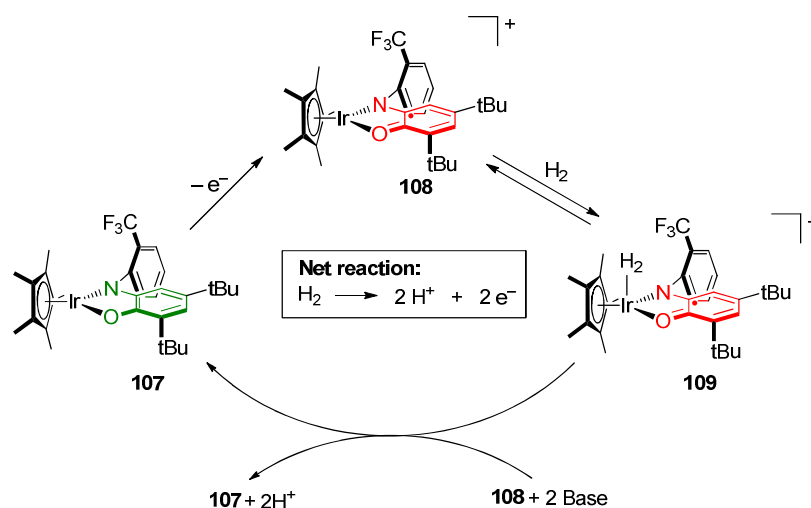
Scheme 38 Reduction of O₂ by a zirconium(IV) complex with a [ONO] pincer ligand.

c) Changing the Lewis acidity/basicity

A change in the oxidation state of a coordinated redox-active ligand can have a significant influence on the Lewis-acidity or -basicity of a metal center. As a result the coordination behavior of a substrate or hemilabile donor can be drastically changed, allowing for redox-switchable catalysis.

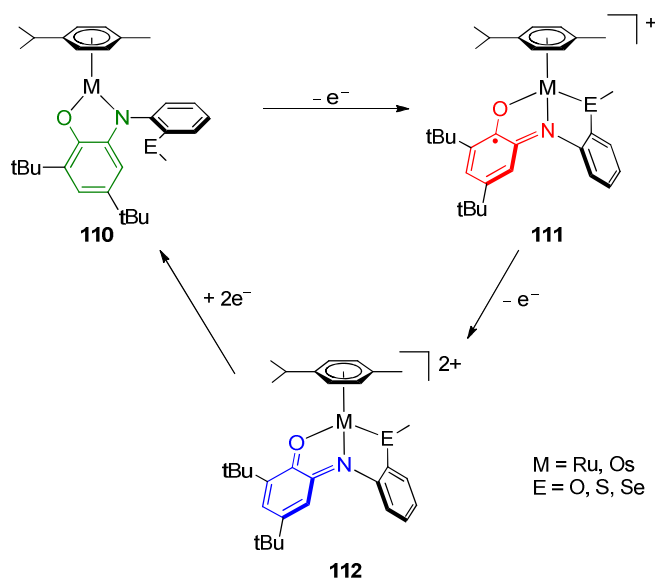
Rauchfuss *et al.* reported redox-switchable iridium complex **107**, containing a redox-active amidophenolato ligand that is capable of catalytically oxidizing dihydrogen (Scheme 39).⁷⁷ Upon one-electron oxidation of the redox-active ligand to form **108**, the Lewis-acidity of the complex is increased, thereby allowing reversible binding of dihydrogen (**109**). In the presence of a base and an oxidant, the complex is capable of oxidizing dihydrogen to protons. Using D₂, a small kinetic isotope

effect of <1.2 was found, consistent with the binding of H_2 (or D_2) to a metal as the rate determining step.⁷⁸ If no base is present, complex **108** will undergo hydrogenolysis to a bis(iridium)trihydride species with release of redox-active ligand. A follow-up study by the same group focussed on the kinetics for the oxidation of H_2 with **108** and related Rh and Ru complexes and with two different ligands– the original version shown in **108** containing *ortho*-(trifluoromethyl)phenyl at nitrogen or a modified one with a *tert*-butyl group at nitrogen.⁷⁹ Iridium complex **108** proved to be the fastest catalyst for dihydrogen oxidation. Furthermore, the counterion was found to have a significant effect on the overall rate. Sarkar *et al.* later found similar reactivity with square planar platinum(II)-based donor-acceptor systems.⁸⁰ Upon oxidation of the redox-active amidophenolate ligand, the Lewis acidity of the Pt center is increased, making the complex reactive for H_2 activation.



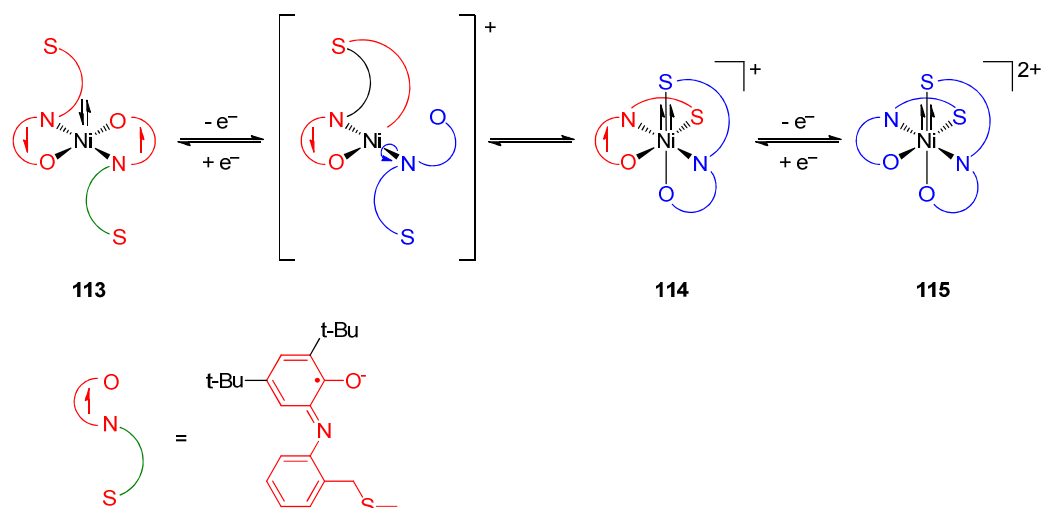
Scheme 39 Redox-switchable Lewis acidity of an iridium complex and its dihydrogen oxidation.

Recently, Kaim *et al.* reported ruthenium and osmium complexes with flexidentate redox-active ligands capable of binding either as bi- or tridentate scaffold. The (E)NO ligand is constructed from an amidophenolate backbone with different weakly coordinating (hemilabile) flanking ether, thioether and selenoether (E) donors (see Scheme 40 for a generic structure of complex **110**).⁸¹ This work builds on earlier research that demonstrated the hemilabile⁸² coordination of a methylthioether group onto iridium depending on the oxidation state of the amidophenolate.⁸³ Upon one-electron oxidation of this (MeS)NO ligand, approximately 8% of the spin density was transferred from the redox-active core of this ligand to the metal, which induces a switch from bidentate NO to tridentate ENO coordination. Not unexpectedly, similar behavior is observed for the other hemilabile (E)NO ligands. This switchable coordination behavior of the ligand is interesting, as the complex changes from a coordinatively unsaturated 16- electron species (**110**) to a coordinatively saturated 18-electron complex (**110**). It can be envisioned that the former may show enhanced (catalytic) reactivity that may be switched off reversibly and on-demand by controlled one-electron ligand oxidation.



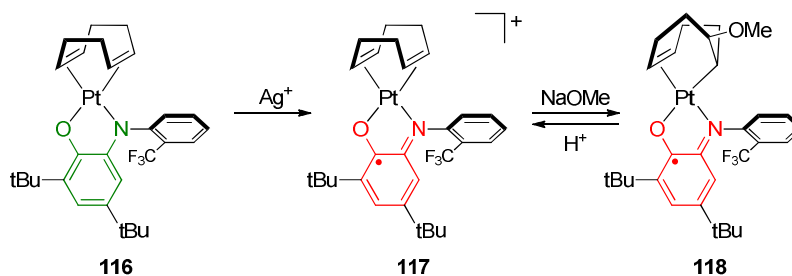
Scheme 40 Redox-switchable hemilabile ligand with ruthenium- or osmium-arene complexes.

Similar redox-dependent hemilabile coordination properties were observed in a homoleptic nickel(II) complex bearing a slightly different redox-active amidophenolate-derived (S)NO ligand with a flanking thioether (Scheme 41).⁸⁴ The starting nickel(II) complex (**113**) has a square planar configuration that lacks any Ni–S bonding and has both oxygen donors in a mutual *trans*-configuration. Upon oxidation by one electron, the two ligands reorient around the Ni-center, results in a mutual *cis* configuration for the O-donors and an overall octahedral geometry around Ni, as both sulfur donors also bind to nickel. One SNO ligand is present in the monoanionic sq^- oxidation state, while the second is bound in the neutral \mathbf{q} oxidation state in species **114**. EPR and magnetic measurements indicate an overall $S = 3/2$ state for this high-spin Ni-system with one ligand-centered radical. Subsequent one-electron oxidation yields the dicationic hexacoordinate nickel(II) complex **114** without any change in coordination mode.



Scheme 41 The conversion of square planar nickel(II) complex **113** to hexacoordinate nickel(II) complex **114** and **115**.

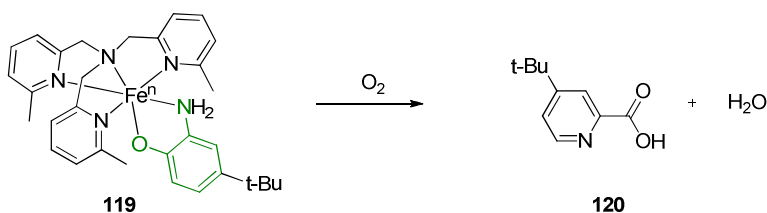
The ability to switch a catalyst on and off by reduction or oxidation is of interest for the design of catalysts that display orthogonal reactivity patterns toward different substrates, allowing for chemoselective conversions and potentially catalytic cascade reactions. A step towards this goal was reported by Rauchfuss and co-workers who showed the redox-switchable activation of coordinated alkenes in a square planar platinum(II) complex with a coordinated redox-active amidophenolate ligand (**116**, Scheme 42).⁸⁵ Cyclic voltammetry showed two fully reversible one-electron oxidation waves at 0.31 V and 1.31 V vs Fc/Fc⁺, indicating that the **sq⁻** and **q** oxidation states of the ligand are both accessible. In the **red²⁻** oxidation state, the coordinated cod ligand is completely unreactive towards nucleophilic attack by e.g. methoxide. However, upon single-electron oxidation by Ag⁺, the diene fragment in **117** rapidly undergoes stereospecific C-O bond formation at the vinylic carbon *trans* to the oxygen donor of the amidophenolate ligand. DFT calculations have indicated that the resulting stereoisomer is in fact the thermodynamically favoured product. Complex **118** was structurally characterized by X-ray crystallography and EPR spectroscopy indicated the presence of a single isomer in solution. The nucleophilic addition proved to be reversible as protonation with HPF₆ regenerated complex **117**.



Scheme 42 Redox-switchable stereospecific methoxide attack on a vinylic carbon of cod coordinated to Pt(II).

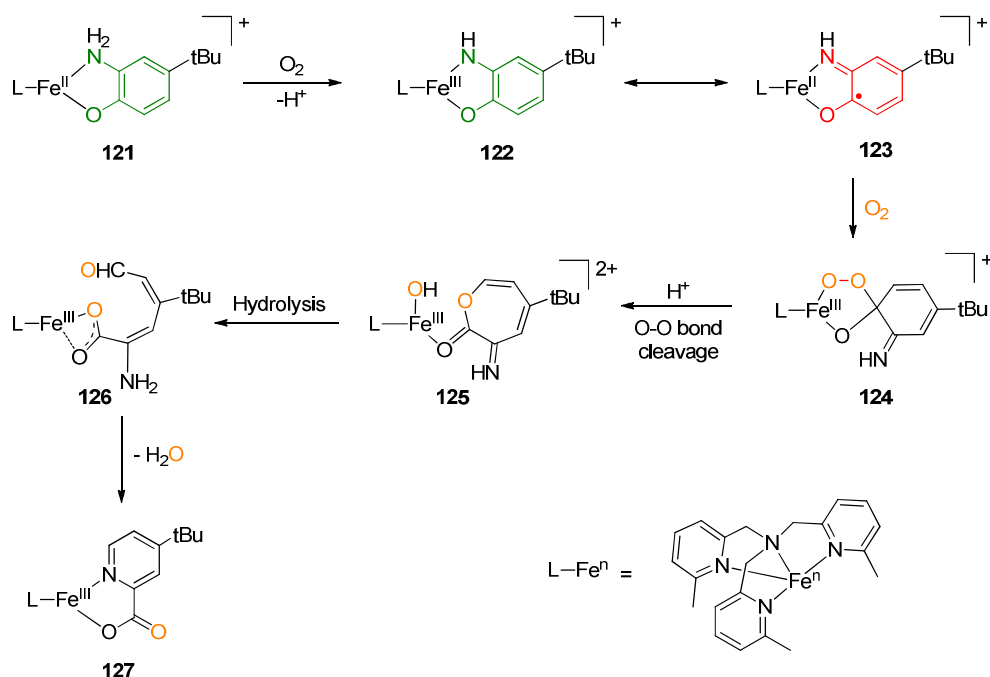
4) Miscellaneous reactivity

Recently, Paine and Chakraborty reported a biomimetic Fe(II) complex (**119**) capable of oxidizing 2-amino-4-*tert*-butylphenol with O₂ (Scheme 43).⁸⁶ This is similar to the activity of dioxygenases occurring in Nature, which are able to catalyze the ring-cleavage of numerous aromatic compounds.⁸⁷ The system is a six-coordinated complex wherein the redox-active aminophenol ligand gets oxidized by O₂ to the corresponding picolinic acid (**120**).



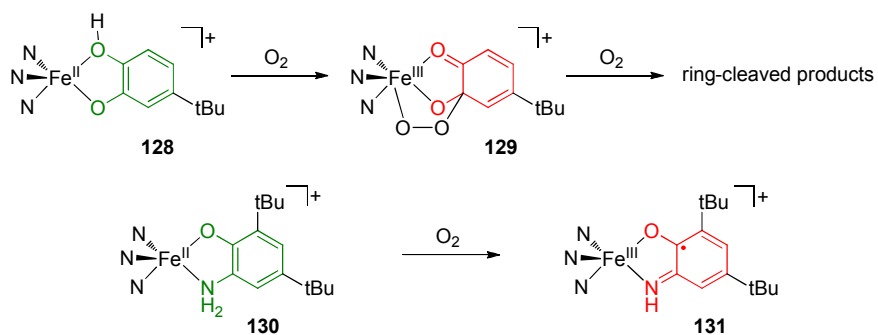
Scheme 43 Net reaction of the oxidative ring cleavage of 2-amino-4-*tert*-butylphenol by the biomimetic Fe(II) complex.

On the basis of findings from this and previous studies, a mechanism was proposed to explain this selectivity (Scheme 44). The first step involves the one-electron oxidation of the *metal* by O₂ to form iron(III) 2-aminophenolate complex **122**. The redox-isomer of this species, iron(II)-2-iminobenzo-semiquinone **123**, featuring a ligand-centered radical at the ON fragment, can react with O₂ to produce alkylperoxo intermediate **124**, with decoordination of the nitrogen donor of the ON fragment. This intermediate undergoes O-O bond cleavage (**125**) followed by hydrolysis to generate aldehyde **126**, which can intramolecularly undergo a condensation reaction with the formed –NH₂ group to give complex **127** bearing the cyclized product 4-*tert*-butyl-2-picolinic acid. These two examples nicely display the necessity to install protective *tert*-butyl groups in the backbone of an aminophenol and at the *nitrogen* substituent to sustain stability of a redox-active ligand-centered radical against aerobic oxidative ring opening.



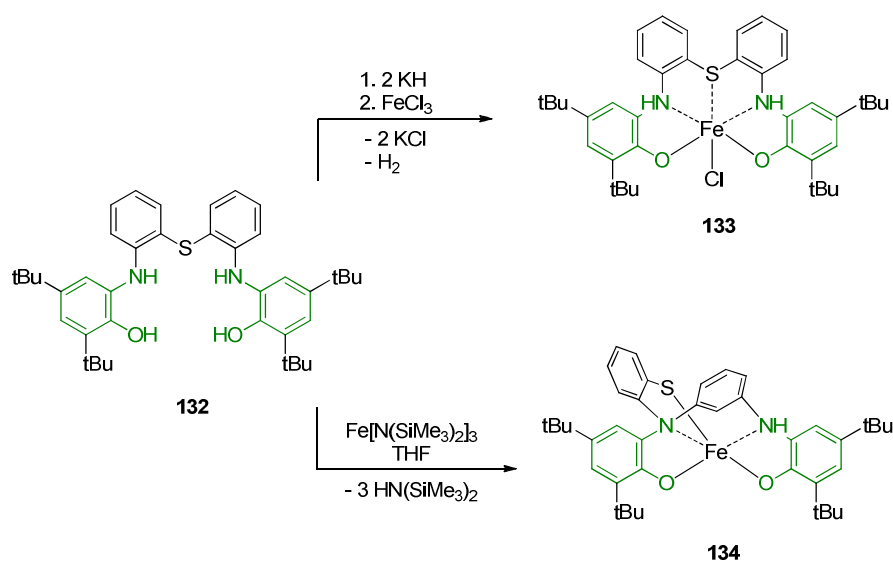
Scheme 44 Proposed mechanism for the oxidative ring cleavage of 2-amino-4-*tert*-butylphenol to the picolinic acid analogue.

Fiedler and co-workers recently demonstrated the necessity to include *tert*-butyl groups at the aminophenolate ring while using a complex with a highly similar coordination environment to the example by Paine and Chakraborty.⁸⁸ In this study, a five-coordinated iron(II) complex was synthesized using the tridentate ligand Ph₂-TIP (*tris*(4,5-diphenyl-1-methylimidazol-2-yl)phosphine) as well as either 4-*tert*-butylcatecholate (OO), 4,6-di-*tert*-butyl-2-aminophenolate (ON) or 4-*tert*-butyl-1,2-phenylenediamine (NN). Although ring-cleavage was observed for the catechol derivative (**128**, Scheme 45), the other two ligands did not suffer from this degradation reaction. Rather, reaction of 2-aminophenol derivative **130** with O₂ results in one-electron oxidation at both the ligand (from **red**²⁻ to **sq**⁻) and the metal (from Fe^{II} to Fe^{III}) to give **131**. This is consistent with the proposed mechanism by Paine and Chakraborty.



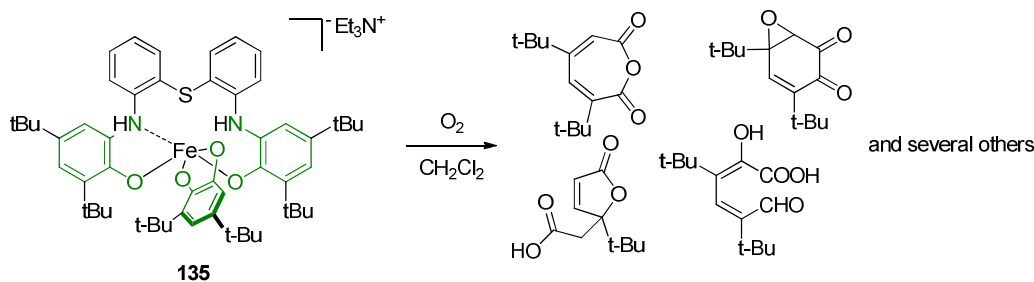
Scheme 45 Different reactivities toward O₂ of Fe(II) complexes with substituted catechol and aminophenol ligands.

An iron(III) complex containing a pentadentate redox-active ONSNO ligand (**132**) that facilitates O₂ reactivity was recently reported by Limberg and co-workers (Scheme 46).⁸⁹ Upon treatment of ligand **132** with KH, to deprotonate the phenol-groups, followed by reaction with FeCl₃ led to the desired complex (**133**) with neutral diphenylamine groups in the bisanionic coordinated ligand. Interestingly, when the precursor ligand was reacted with Fe(N(SiMe₃)₂)₃, ligand rearrangement via C–S bond cleavage occurred to form complex **134**.



Scheme 46 Synthesis of pentadentate O,N,S,N,O-ligand Fe(III) complexes.

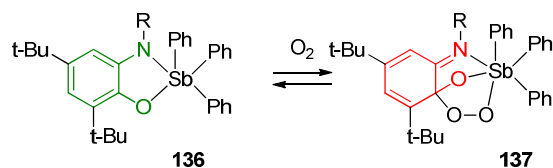
Both complexes **133** and **134** reacted with O₂ to give oxidation of the two redox-active moieties to the sq^- oxidation states with concomitant formation of H₂O₂. More interestingly, upon treatment of complex **129** with 3,5-di-*tert*-butylcatechol in the presence of triethylamine, complex **135** was obtained selectively (Scheme 47). Follow-up exposure to dioxygen resulted in ring-cleavage reactivity at the catechol fragment to give a broad palette of different ring-cleavage products. Further studies are required to determine the mechanism of this reaction and the exact involvement of the redox-active ONSNO ligand.



Scheme 47 Ring cleavage upon reaction of **135** with O₂.

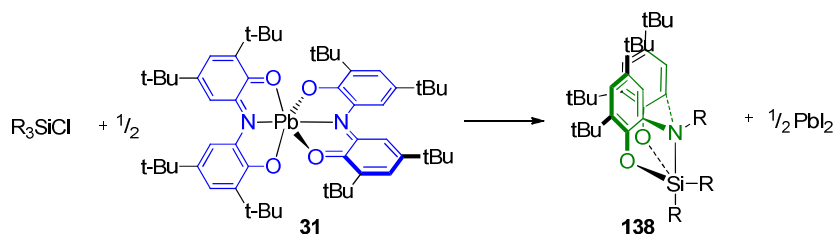
Palaniandavar *et al.* reported a number of complexes bearing either a tridentate NNN,⁹⁰ tetradentate NNNN⁹¹ or tetradentate ONNN ligand⁹² in combination with iron(III) for related biomimetic oxidation studies of 3,5-di-*tert*-butylcatechol. These reactions generally led to the same products as shown in Scheme 45, although the product distribution differs per system.

The first example of reversible binding of O₂ to a non-transition metal (antimony(V)) facilitated by a redox-active *o*-amidophenolato ligand was reported by Abakumov and co-workers (Scheme 48).⁹³ The group found that complex **136**, which is air-stable as a solid, reacts with O₂ in solution to form spiroendoperoxide **137**. Both complexes were isolated and structurally characterized. Interestingly, upon moderate heating, species **137** converted back to the starting material by elimination of O₂. The influence of steric and electronic factors on the reversible O₂ binding was reported by the same group.⁹⁴



Scheme 48 Reversible binding of O₂ to an *o*-amidophenolato (X = N) antimony(V) complex.

The group of Brown reported the migration of alkyl and aryl groups from silicon to the nitrogen of a redox active ONO ligand in silylated aryloxyiminoquinones.⁹⁵ A reaction between methyl and phenyl substituted chlorosilanes and complex **31** readily affords five-coordinated silanes (**138**) ligated to a tridentate, dianionic ONO ligand (Scheme 49). Compound **138** is formed by two-electron reduction and alkyl or aryl group migration to nitrogen. Notably, when chlorosilanes bearing both methyl and phenyl groups were used, exclusively methyl migration was observed. More recently the group reported a mechanistic investigation to elucidate the mechanism and explain the reactivity.⁹⁶ Cross-over experiments using (CH₃)₃SiCl and (CD₃)₃SiCl showed that the migration occurs in an intramolecular fashion. DFT calculations suggested that the origin for the exclusive selectivity of methyl migration is due to the faster formation of one of the possible octahedral intermediates and that migration occurs faster than isomerization.



Scheme 49 Alkyl and aryl migration from silicon to nitrogen. R = Me or Ph.

5) Conclusions

The application of redox-active ligands, which have traditionally been considered as mainly a spectroscopic curiosity in coordination chemistry, to expand the existing or to induce new reactivity at transition, rare earth and main group metal complexes is a flourishing field of research. With a focus on the three closely related classes derived from catechol, *o*-aminophenol or *o*-phenylenediamine, a representative overview of the main current strategies to exploit redox-active ligands in stoichiometric and catalytic processes are illustrated. The main premise of many of these applications is the facile *reversible* ligand-based redox-shuttling events that can be addressed in a controlled manner. The main ‘mode of operation’ for these systems is as electron reservoir for the activation of specific substrate bonds or the coupling of two reagents. Depending on the starting oxidation state of the ligand framework, which span from doubly reduced **red**²⁻ via mono-reduced-mono-oxidized **isq**⁻ to doubly oxidized **q**, up to two electrons could be harbored or released by these organic entities. Commonly, one-electron redox-shuttling is observed for each ligand under the specific reaction conditions. Hence, many of the initial research exploit bis-ligated metal complexes to combine two ligand-based single-electron transfer processes. These constructs allow to mimic ‘classic’ two-electron transfer reactivity, traditionally observed for noble metals, at high-valent early transition metal *d*⁰ complexes that lack redox-equivalents at the metal center to facilitate e.g. oxidative addition processes. However, there is a growing number of elegant examples where redox-active ligands can expand the reactivity in the first coordination sphere of a metal center by acting as more than just an electron reservoir. One promising concept utilizes direct intramolecular ligand-to-substrate single-electron transfer to generate and stabilize metal-bound substrate-centered. The combination of this new approach with metals that commonly do not display odd-electron radical-type reactivity (e.g. closed-shell 2nd and 3rd row late transition metal ions) allows for unprecedented new reactivity modes. Addressing the different oxidation states available in a redox-active ligand manifold can also be effectively used to change the Lewis acidity of a metal. This may induce reversible geometric changes around the metal center, alter the binding affinity toward substrates or activate coordinated substrates for reaction with exogenous reactants. It also may enable redox-switchable (catalytic) reactivity. Lastly, redox-active ligands may also demonstrate chemoresponsive behavior, wherein the ligand actively participates in bond-making and -breaking processes. To date, these strategies have been mainly demonstrated in stoichiometric conversions, although several catalytic transformations by virtue of redox-active ligand systems has already been achieved, albeit with moderate activity in most cases. However, it is believed to be only a matter of time before redox-active ligand systems will become a mainstream strategy for homogeneous catalysis, in large part thanks to the highly tunable character of reactive entities based on catechol, *o*-aminophenol or *o*-phenylenediamine. The combination of these ligand systems with base metals is expected to allow mimicking of classic noble-metal catalysis. The unique opportunities created by combining the well-known (organometallic) coordination chemistry of

closed-shell noble metal ions with ligand-induced odd-electron reactivity also promise to deliver unprecedented reactivity, unattainable using traditional metal-ligand combinations. Although there is likely no “one-size-fits-all” redox-active ligand concept, exciting new types of catalytic reactivity and novel applications of these redox-active ligands will definitely appear in the foreseeable future.

6) Acknowledgements

Our own research in the area of redox-active and reactive ligands for bond activation and small molecule functionalization is funded by the European Research Council through an ERC Starting Grant (Agreement 279097, *EuReCat*) to J.I.v.d.V. We thank profs de Bruin and Reek (both Univ. of Amsterdam) for fruitful scientific discussions and collaborative research.

7) References

- ¹ C. C. C. Johansson Seechurn, M. O. Kitching, T. J. Colacot and V. Snieckus, *Angew. Chem. Int. Ed.*, 2012, **51**, 5062-5085.
- ² M. Beller, A. Renken and R. A. van Santen, *Catalysis, From Principles to Applications*, Eds, Wiley-VCH, 2012; R. H. Crabtree, *The Organometallic Chemistry of the Transition Metals*, 5th edn, Wiley, 2009.
- ³ W. I. Dzik, J. I. van der Vlugt, J. N. H. Reek and B. de Bruin, *Angew. Chem. Int. Ed.*, 2011, **50**, 3356-3358; b), J. I. van der Vlugt, *Eur. J. Inorg. Chem.*, 2012, 363-375; V. Lyaskovskyy and B. de Bruin *ACS Catal.*, 2012, **2**, 270-279; V. K. K. Praneeth, M. R. Ringenberg and T. R. Ward, *Angew. Chem. Int. Ed.*, 2012, **51**, 10228-10234; O. R. Luca and R. H. Crabtree, *Chem. Soc. Rev.*, 2013, **42**, 1440-1459.
- ⁴ P. J. Chirik and K. Wieghardt, *Science*, 2010, **327**, 794-795.
- ⁵ a) J. Stubbe and W. A. van der Donk, *Chem. Rev.*, 1998, **98**, 705-762; b) W. Kaim and B. Schwederski, *Coord. Chem. Rev.*, 2010, **254**, 1580-1588.
- ⁶ For a historic perspective, see: R. Eisenberg and H. B. Gray, *Inorg. Chem.*, 2011, **50**, 9741-9751; P. Chirik, *Inorg. Chem.*, 2011, **50**, 9737-9740; W. Kaim and B. Schwederski, *Coord. Chem. Rev.* 2010, **254**, 1580-1588; S. Sproules, K. Wieghardt, *Coord. Chem. Rev.* 2010, **254**, 1358-1382; S. Sproules, K. Wieghardt, *Coord. Chem. Rev.* 2010, **255**, 837-860; C. G. Pierpont and C. W. Lange, *Progr. Inorg. Chem.* 1994, **41**, 331-442; C. G. Pierpont and R. M. Buchanan, *Coord. Chem. Rev.* 1981, **38**, 45-87.
- ⁷ W. I. Dzik, X. P. Zhang and B. de Bruin, *Inorg. Chem.*, 2011, **50**, 9896-9903.
- ⁸ T. Diao, P. J. Chirik, A. K. Roy, K. Lewis, S. A. Nye, K. J. Weller, J. G. P. Delis, R. Yu, US Pat. 20150080536A1; K. M. Lewis, C. C. Hojila Atienza, J. L. Boyer, P. J. Chirik, J. G. P. Delis, A. K. Roy, US Pat. 20140330036A1; A. M. Tondreau, P. J. Chirik, J. G. P. Delis, K. J. Weller, K. Lewis, S. A. Nye, US Pat. 20120130021A1.
- ⁹ D. M. Connor, K. A. Keller and J. G. Lever, US 20070113967; W. Sato, T. Nakamura, M. Takeuchi and S. Maeda, JP 2007015181; W. Sato, K. Okamoto, Y. Saito, M. Kawashima and T. Kaneda, WO 2006118277; Y. Saito, I. Sato and H. Morii, JP 2006195399.
- ¹⁰ Catechol: C. G. Pierpont, *Coord. Chem. Rev.*, 2001, **219-221**, 415-433; C. G. Pierpont, *Coord. Chem. Rev.*, 2001, **216-217**, 99-125; C. G. Pierpont, *Inorg. Chem.*, 2011, **50**, 9766-9772.
- ¹¹ Aminophenol: A. I. Poddel'sky, V. K. Cherkasov and G. A. Abakumov, *Coord. Chem. Rev.*, 2009, **253**, 291-324.
- ¹² *o*-phenylenediamine: A. Mederos, S. Domínguez, R. Hernández-Molina, J. Sanchiz and F. Brito, *Coord. Chem. Rev.*, 1999, **193-195**, 913-939.
- ¹³ G. Skara, B. Pinter, P. Geerlings and F. De Proft, *Chem. Sci.* 2015, **6**, 4109-4117.
- ¹⁴ S. Kokatam, T. Weyhermüller, E. Bothe, P. Chaudhure and K. Wieghardt, *Inorg. Chem.*, 2005, **44**, 3709-3717.
- ¹⁵ S. N. Brown, *Inorg. Chem.*, 2012, **51**, 1251-1260
- ¹⁶ W. Kaim and A. Klein, *Spectroelectrochemistry*, Royal Society of Chemistry; 1st edn, 2008.
- ¹⁷ K. Ray, T. Petrenko, K. Wieghardt and F. Neese, *Dalton Trans.*, 2007, 1552-1566.
- ¹⁸ W. Kaim, *Inorg. Chem.*, 2011, **50**, 9752-9765.
- ¹⁹ C. K. Jørgensen, *Coord. Chem. Rev.*, 1966, **1**, 164-178

-
- ²⁰ R. F. Munhá, R. A. Zarkesh and A. F. Heyduk, *Inorg. Chem.*, 2013, **52**, 11244-11255.
- ²¹ K. J. Blackmore, J. W. Ziller and A. F. Heyduk *Inorg. Chem.*, 2005, **44**, 5559-5561.
- ²² M. R. Haneline and A. F. Heyduk, *J. Am. Chem. Soc.*, 2006, **128**, 8410-8411.
- ²³ G. Szigethy and A. F. Heyduk, *Inorg. Chem.*, 2011, **50**, 125-135.
- ²⁴ R. A. Zarkesh, J. W. Ziller and A. F. Heyduk, *Angew. Chem. Int. Ed.*, 2008, **47**, 4715-4718.
- ²⁵ R. A. Zarkesh and A. F. Heyduk, *Organometallics* 2011, **30**, 4890-4898.
- ²⁶ R. A. Zarkesh and A. F. Heyduk, *Organometallics* 2009, **28**, 6629-6631.
- ²⁷ A. F. Heyduk, R. A. Zarkesh and A. I. Nguyen, *Inorg. Chem.*, 2011, **50**, 9849-9863.
- ²⁸ A. I. Nguyen, K. J. Blackmore, S. M. Carter, R. A. Zarkesh and A. F. Heyduk, *J. Am. Chem. Soc.*, 2009, **131**, 3307-3316.
- ²⁹ R. F. Munhá, R. A. Zarkesh and A. F. Heyduk, *Dalton. Trans.*, 2013, **42**, 3751-3766.
- ³⁰ A. I. Nguyen, R. A. Zarkesh, D. C. Lacy, M. K. Thorson and A. F. Heyduk, *Chem. Sci.*, 2011, **2**, 166-169.
- ³¹ S. Ghosh and M. -H. Baik, *Chem. Eur. J.*, 2015, **21**, 1780-1789
- ³² K. J. Blackmore, N. Lal, J. W. Ziller and A. F. Heyduk, *J. Am. Chem. Soc.*, 2008, **130**, 2728-2729.
- ³³ K. J. Blackmore, N. Lal, J. W. Ziller and A. F. Heyduk, *Eur. J. Inorg. Chem.*, 2009, 735-743.
- ³⁴ N. A. Ketterer, H. Fan, K. J. Blackmore, X. Yang, J. W. Ziller, M. Baik and A. F. Heyduk, *J. Am. Chem. Soc.*, 2008, **130**, 4364-4374.
- ³⁵ S. Hananouchi, B. T. Krull, J. W. Ziller, F. Furche and A. F. Heyduk *Dalton Trans.*, 2014, **43**, 17991-18000.
- ³⁶ R. A. Holm, *Chem. Rev.*, 1987, **87**, 1401-1449.
- ³⁷ R. Marshall-Roth, S. C. Liebscher, K. Rickert, N. J. Seewald, A. G. Oliver and S. N. Brown, *Chem. Commun.*, 2012, **48**, 7826-7828.
- ³⁸ A. H. Randolph, N. J. Seewald, K. Rickert and S. N. Brown, *Inorg. Chem.*, 2013, **52**, 12587-12598.
- ³⁹ D. D. Wright and S. N. Brown, *Inorg. Chem.*, 2013, **52**, 7831-7833.
- ⁴⁰ B. R. McGarvey, A. Ozarowski, Z. Tian and D. G. Tuck, *Can. J. Chem.*, 1995, **73**, 1213-1222.
- ⁴¹ Selected examples: P. Chaudhuri, C. N. Verani, E. Bill, E. Bothe, T. Weyhermüller and K. Wieghardt *J. Am. Chem. Soc.*, 2001, **123**, 2213-2223; H. Chun, C. N. Verani, P. Chaudhuri, E. Bothe, E. Bill, T. Weyhermüller and K. Wieghardt, *Inorg. Chem.*, 2001, 4157-4166; V. Bachler, G. Olbrich, F. Neese, and K. Wieghardt, *Inorg. Chem.*, 2002, **41**, 4179-4193; S. Sun, H. Chun, K. Hildenbrand, E. Bothe, T. Weyhermüller, F. Neese, F and K. Wieghardt, *Inorg. Chem.*, 2002, **41**, 4295-4303; H. Chun, E. Bill, E. Bothe, T. Weyhermüller and K. Wieghardt, *Inorg. Chem.*, 2002, **41**, 493-499; H. Chun, E. Bill, T. Weyhermüller and K. Wieghardt *Inorg. Chem.*, 2003, **42**, 5612-5620; K. S. Min, T. Weyhermüller, E. Bothe and K. Wieghardt, *Inorg. Chem.*, 2004, **43**, 2922-2931; K. S. Min, T. Weyhermüller and K. Wieghardt, *Dalton Trans.*, 2004, 178-186.
- ⁴² T. Wada, K. Tsuge and K. Tanaka, *Inorg. Chem.*, 2001, **40**, 329-337.

- ⁴³ J. T. Muckerman, D. E. Polyansky, T. Wada, K. Tanaka and E. Fujita, *Inorg. Chem.*, 2008, **47**, 1787–1802; S. Ghosh and M. Baik, *Inorg. Chem.*, 2011, **50**, 5946–5957; H. Isobe, K. Tanaka, J.-R. Shen and K. Yamaguchi, *Inorg. Chem.*, 2014, **53**, 3973–3984.
- ⁴⁴ T. Matsumoto, H. Chang, M. Wakizaka, S. Ueno, A. Kobayashi, A. Nakayama, T. Taketsugu, and M. Kato, *J. Am. Chem. Soc.*, 2013, **135**, 8646–8654.
- ⁴⁵ J. L. Wong, R. Hernández Sánchez, J. Glancy Logan, R. A. Zarkesh, J. W. Ziller and A. F. Heyduk, *Chem. Sci.*, 2013, **4**, 1906–1910
- ⁴⁶ A. L. Smith, K. I. Hardcastle and J. D. Soper, *J. Am. Chem. Soc.*, 2010, **132**, 14358–14360.
- ⁴⁷ M. van der Meer, Y. Rechkemmer, I. Peremykin, S. Hohloch, J. van Slageren and B. Sarkar, *Chem. Commun.*, 2014, **50**, 11104–11106.
- ⁴⁸ C. Mukherjee, T. Weyhermüller, E. Bothe and P. Chaudhuri, *Inorg. Chem.*, 2008, **47**, 2740–2746.
- ⁴⁹ J. Jacquet, E. Salanouve, M. Orio, H. Vezin, S. Blanchard, E. Derat, M. Desage-El Murr and L. Fensterbank, *Chem. Commun.*, 2014, **50**, 10394–10397.
- ⁵⁰ T. Umemoto *Chem. Rev.*, 1996, **96**, 1757–1778; H. Li *Synlett*, 2012, **23**, 2289–2290
- ⁵¹ C. Mukherjee, T. Weyhermüller, E. Bothe, E. Rentschler and P. Chaudhuri, *Inorg. Chem.*, 2007, **46**, 9895–9905.
- ⁵² A. V. Piskunov, I. V. Ershova, G. K. Fukin, A. S. Shavyrin, *Inorg. Chem. Commun.*, 2013, **38**, 127–130.
- ⁵³ A. V. Piskunov, I. N. Meshcheryakova, G. K. Fukin, A. S. Shavyrin, V. K. Cherkasov and G. A. Abakumov, *Dalton Trans.*, 2013, **42**, 10533–10539.
- ⁵⁴ E. M. Matson, S. M. Franke, N. H. Anderson, T. D. Cook, P. E. Fanwick and S. C. Bart, *Organometallics*, 2014, **33**, 1964–1971.
- ⁵⁵ E. M. Matson, S. R. Opperwall, P. E. Fanwick and S. C. Bart, *Inorg. Chem.*, 2013, **52**, 7295–7304.
- ⁵⁶ W. Zhou, B. O. Patrick and K. M. Smith, *Chem. Commun.* 2014, **50**, 9958–9960.
- ⁵⁷ C. A. Lippert, S. A. Arnstein, C. D. Sherrill and J. D. Soper, *J. Am. Chem. Soc.*, 2010, **132**, 3879–3892.
- ⁵⁸ R. H. Holm, *Chem. Rev.*, 1987, **87**, 1401–1449; B. G. Jacobi, D. S. Laitar, L. Pu, M. F. Wargocki, A. G. DiPasquale, K. C. Fortner, S. M. Schuck and S. N. Brown, *Inorg. Chem.*, 2002, **41**, 4815–4823; E. Harlan, J. M. Berg and R. H. Holm, *J. Am. Chem. Soc.*, 1986, **108**, 6992–7000; S. N. Brown and J. M. Mayer, *Inorg. Chem.*, 1993, **31**, 1988–1993.
- ⁵⁹ J. H. Espenson, *Adv. Inorg. Chem.*, 2003, **54**, 157–202.
- ⁶⁰ C. A. Lippert and J. D. Soper, *Inorg. Chem.*, 2010, **49**, 3682–3684.
- ⁶¹ C. A. Lippert, K. Riener and J. D. Soper, *Eur. J. Inorg. Chem.* 2012, 554–561.
- ⁶² C. A. Lippert, K. I. Hardcastle and J. D. Soper, *Inorg. Chem.*, 2011, **50**, 9864–9878.
- ⁶³ D. L. J. Broere, B. de Bruin, J. N. H. Reek, M. Lutz, S. Dechert and J. I. van der Vlugt, *J. Am. Chem. Soc.*, 2014, **136**, 11574–11577.
- ⁶⁴ Further investigated in: D. L. J. Broere, S. Demeshko, B. de Bruin, E. A. Pidko, J. N. H. Reek, M. A. Siegler, M. Lutz and J. I. van der Vlugt, *Chem. Eur. J.*, 2015, **21**, 5879–5886.

- ⁶⁵ A. Hedström, Z. Izakian, I. Vreto, C.-J. Wallentin and P.-O. Norrby, *Chem. Eur. J.* 2015, **21**, 5946–5953; E. T. Hennessy, R. Y. Liu, D. A. Iovan, R. A. Duncan and T. A. Betley, *Chem. Sci.*, 2014, **5**, 1526–1532; N. D. Paul, S. Mandal, M. Otte, X. Cui, X. P. Zhang and B. de Bruin *J. Am. Chem. Soc.*, 2014, **136**, 1090; E. T. Hennessy, T. A. Betley *Science* **2013**, *340*, 591; N. D. Paul, A. Chirila, H. Lu, X. P. Zhang and B. de Bruin, *Chem. Eur. J.* 2013, **19**, 12953; C. T. To, K. S. Choi, K. S. Chan, *J. Am. Chem. Soc.* 2012, **134**, 11388–11391; B. de Bruin, W. I. Dzik, S. Li and B. B. Wayland, *Chem. Eur. J.* 2009, **15**, 4312–4320; K. Satoh and M. Kamigaito, *Chem. Rev.* 2009, **109**, 5120–5156.
- ⁶⁶ D. L. J. Broere, L. L. Metz, B. de Bruin, J. N. H. Reek, M. A. Siegler and J. I. van der Vlugt, *Angew. Chem. Int. Ed.*, 2015, **54**, 1516–1520.
- ⁶⁷ General reviews: R. H. Morris, *Acc. Chem. Res.*, 2015, **48**, 1494–1502; H. Li, B. Zheng and K.-W. Huang, *Coord. Chem. Rev.*, 2015, **293–294**, 116–138; C. Gunanathan and D. Milstein, *Chem. Rev.*, 2014, **114**, 12024–12087; H. A. Younus, N. Ahmad, W. Su and F. Verpoort, *Coord. Chem. Rev.*, 2014, **276**, 112–152; S. Kuwata and T. Ikariya, *Chem. Commun.*, 2014, **50**, 14290–14300; B. Zhao, Z. Han and K. Ding, *Angew. Chem. Int. Ed.*, 2013, **52**, 4744; W.-H. Wang, J. T. Muckerman, E. Fujita and Y. Himeda, *New J. Chem.*, 2013, **37**, 1860; S. Schneider, J. Meiners and B. Askevold, *Eur. J. Inorg. Chem.*, 2012, 412; T. Ikariya, *Top. Organomet. Chem.*, 2011, **37**, 31; C. Gunanathan and D. Milstein, *Acc. Chem. Res.*, 2011, **44**, 588; D. Milstein, *Top. Catal.*, 2010, **53**, 915; J. I. van der Vlugt and J. N. H. Reek, *Angew. Chem. Int. Ed.*, 2009, **48**, 8832–8846; D. Gelman and S. Musa, *ACS Catal.* 2012, **2**, 2456–2466; D. Benito-Garagorri and K. Kirchner, *Acc. Chem. Res.* 2008, **41**, 201–213; T. Ikariya, K. Murata, R. Noyori, *Org. Biomol. Chem.* 2006, 393–406; D. B. Grotjahn, *Chem. Eur. J.* 2005, **11**, 7146–7153.
- ⁶⁸ Examples from our own group: J. I. van der Vlugt, E. A. Pidko, M. Lutz, D. Vogt and A. L. Spek, *Dalton Trans.*, 2009, 1016–1023; J. I. van der Vlugt, M. A. Siegler, M. Janssen, D. Vogt and A. L. Spek, *Organometallics*, 2009, **28**, 7025–7032; J. I. van der Vlugt, E. A. Pidko, R. C. Bauer, Y. Gloaguen, M. K. Rong and M. Lutz, *Chem. Eur. J.*, 2011, **17**, 3850–3854; R. C. Bauer, Y. Gloaguen, M. Lutz, J. N. H. Reek, B. de Bruin and J. I. van der Vlugt, *Dalton Trans.*, 2011, **40**, 8822–8829; S. Y. de Boer, Y. Gloaguen, M. Lutz and J. I. van der Vlugt, *Inorg. Chim. Acta*, 2012, **380**, 336–342; S. Y. de Boer, Y. Gloaguen, J. N. H. Reek, M. Lutz and J. I. van der Vlugt, *Dalton Trans.*, 2012, **41**, 11276–11283; Y. Gloaguen, W. Jacobs, B. de Bruin, M. Lutz and J. I. van der Vlugt, *Inorg. Chem.*, 2013, **52**, 1682 – 1684; Y. Gloaguen, L. M. Jongens, M. Lutz, J. N. H. Reek, B. de Bruin and J. I. van der Vlugt, *Organometallics*, 2013, **32**, 4284–4291; F. G. Terrade, M. Lutz, J. I. van der Vlugt, J. N. H. Reek, *Eur. J. Inorg. Chem.*, 2014, 1826–1835; L. S. Jongbloed, B. de Bruin, J. N. H. Reek, M. Lutz and J. I. van der Vlugt, *Chem. Eur. J.*, 2015, **21**, 7297–7305; S. Oldenhof, F. G. Terrade, M. Lutz, J. I. van der Vlugt and J. N. H. Reek, *Organometallics*, 2015, **34**, 10.1021/acs.organomet.5b00249; Z. Tang, E. Otten, J. N. H. Reek, J. I. van der Vlugt and B. de Bruin, *Chem. Eur. J.*, 2015, **21**, doi: 10.1002/chem.201501453.
- ⁶⁹ P. Chaudhuri, M. Hess, J. Mu, K. Hildenbrand, E. Bill and K. Wieghardt, *J. Am. Chem. Soc.*, 1999, **121**, 9599–9610.
- ⁷⁰ J. W. Whittaker, In *Metal Ions in Biological Systems*; Sigel, H., Sigel, A., Eds.; Marcel Dekker: New York, 1994; Vol. 30, pp 315–360.
- ⁷¹ S. E. Balaghi, E. Safaei, L. Chiang, E. W. Y. Wong, D. Savard, R. M. Clarke and T. Storr, *Dalton Trans.*, **42**, 6829–6839; Z. Alaji, E. Safaei, L. Chiang, R. M. Clarke, C. Mu and T. Storr, *Eur. J. Inorg. Chem.*, 2014, 6066–6074.
- ⁷² H. Ozawa, T. Hino, H. Ohtsu, T. Wada and K. Tanaka, *Inorg. Chim. Acta*, 2011, **366**, 298–302.
- ⁷³ Y. Miyazato, T. Wada, J. T. Muckerman, E. Fujita and K. Tanaka, *Angew. Chem. Int. Ed.*, 2007, **46**, 5728–5730.
- ⁷⁴ J. L. Boyer, J. Rochford, M.-K. Tsai, J. T. Muckerman and E. Fujita, *Coord. Chem. Rev.*, 2010, **254**, 309–330.
- ⁷⁵ F. Lu, R. A. Zarkesh and A. F. Heyduk, *Eur. J. Inorg. Chem.*, 2012, 467–470.
- ⁷⁶ J. J. Warren, T. A. Tronic and J. M. Mayer, *Chem. Rev.*, 2010, **110**, 6961–7001; J. M. Mayer, *Acc. Chem. Res.*, 2011, **44**, 36–46.

-
- ⁷⁷ M. R. Ringenberg, S. L. Kokatam, Z. M. Heiden and T. B. Rauchfuss, *J. Am. Chem. Soc.*, 2008, **130**, 788–789.
- ⁷⁸ K. Zhang, C. D. Hoff and A. A. Gonzalez, *J. Am. Chem. Soc.*, 1989, **111**, 3627–3632.
- ⁷⁹ M. R. Ringenberg, M. J. Nilges, T. B. Rauchfuss and S. R. Wilson, *Organometallics* 2010, **29**, 1956–1965.
- ⁸⁰ N. Deibel, D. Schweinfurth, S. Hohloch, J. Fiedler and B. Sarkar, *Chem. Commun.*, 2012, **48**, 2388–2390.
- ⁸¹ M. Bubrin, D. Schweinfurth, F. Ehret, S. Záliš, H. Kvapilová, J. Fiedler, Q. Zeng, F. Hartl and W. Kaim, *Organometallics*, 2014, **33**, 4973–4985.
- ⁸² R. Lindner, B. van den Bosch, M. Lutz, J. N. H. Reek and J. I. van der Vlugt, *Organometallics*, 2011, **30**, 499–510.
- ⁸³ R. Hübner, S. Weber, S. Strobel, B. Sarkar, S. Záliš and W. Kaim, *Organometallics*, 2011, **30**, 1414–1418.
- ⁸⁴ A. Paretzki, M. Bubrin, J. Fiedler, S. Záliš and W. Kaim, *Chem. Eur. J.*, 2014, **20**, 5414–5422.
- ⁸⁵ J. L. Boyer, T. R. Cundari, N. J. DeYonker, T. B. Rauchfuss and S. R. Wilson, *Inorg. Chem.*, 2009, **48**, 638–645.
- ⁸⁶ B. Chakraborty and T. K. Paine, *Angew. Chem. Int. Ed.*, 2013, **52**, 920–924.
- ⁸⁷ F. H. Vaillancourt, J. T. Bolin and L. D. Eltis, *Crit. Rev. Biochem. Mol. Biol.*, 2006, **41**, 241–267; L. Que, *Chem. Rev.* 2004, **104**, 939–986; J. D. Lipscomb, *Curr. Opin. Struct. Biol.*, 2008, **18**, 644–649; S. Fetzner, *Appl. Environ. Microbiol.*, 2012, **78**, 2505–2514; G. Fuchs, M. Boll and J. Heider, *Nat. Rev. Microbiol.* 2011, **9**, 803–816.
- ⁸⁸ M. M. Bittner, S. V. Lindeman, C. V. Popescu and A. T. Fiedler, *Inorg. Chem.*, 2014, **53**, 4047–4061.
- ⁸⁹ R. Metzinger, S. Demeshko and C. Limberg, *Chem. Eur. J.*, 2014, **20**, 4721–4735.
- ⁹⁰ M. Sankaralingam, N. Saravanan, N. Anitha, E. Suresh and M. Palaniandavar, *Dalton Trans.*, 2014, **43**, 6828–6841.
- ⁹¹ M. Balamurugan, P. Vadivelu and M. Palaniandavar, *Dalton Trans.*, 2014, **43**, 14653–14668.
- ⁹² R. Mayilmurugan, K. Visvaganesan, E. Suresh and M. Palaniandavar, *Inorg. Chem.*, 2009, **48**, 8771–8783.
- ⁹³ G. A. Abakumov, A. I. Poddel'sky, E. V. Grunova, V. K. Cherkasov, G. K. Fukin, Y. A. Kurskii and L. G. Abakumova, *Angew. Chem. Int. Ed.*, 2005, **44**, 2767–2771.
- ⁹⁴ G. K. Fukin, E. V. Baranov, A. I. Poddel'sky, V. K. Cherkasov and G. A. Abakumov, *ChemPhysChem*, 2012, **13**, 3773–3776.
- ⁹⁵ S. Shekar and S. N. Brown, *Organometallics*, 2013, **32**, 556–564
- ⁹⁶ S. Shekar and S. N. Brown, *J. Org. Chem.*, 2014, **79**, 12047–12055